Check for updates

Advancing piezoelectric 2D nanomaterials for applications in drug delivery systems and therapeutic approaches

Anshuo Li, [ID] †[ab] Jiawei Yang,†[a] Yuchu He,[b] Jin Wen*[a] and Xinquan Jiang*[a]

Precision drug delivery and multimodal synergistic therapy are crucial in treating diverse ailments, such as cancer, tissue damage, and degenerative diseases. Electrodes that emit electric pulses have proven effective in enhancing molecule release and permeability in drug delivery systems. Moreover, the physiological electrical microenvironment plays a vital role in regulating biological functions and triggering action potentials in neural and muscular tissues. Due to their unique noncentrosymmetric structures, many 2D materials exhibit outstanding piezoelectric performance, generating positive and negative charges under mechanical forces. This ability facilitates precise drug targeting and ensures high stimulus responsiveness, thereby controlling cellular destinies. Additionally, the abundant active sites within piezoelectric 2D materials facilitate efficient catalysis through piezochemical coupling, offering multimodal synergistic therapeutic strategies. However, the full potential of piezoelectric 2D nanomaterials in drug delivery system design remains underexplored due to research gaps. In this context, the current applications of piezoelectric 2D materials in disease management are summarized in this review, and the development of drug delivery systems influenced by these materials is forecast.

1 Introduction

At present, an estimated 90% of pharmaceuticals are administered orally, yet they frequently exhibit suboptimal efficacy.[1] In response, there has been a concerted effort to develop sophisticated drug delivery systems aimed at augmenting treatment effectiveness.[2] This development often incorporates additional physical stimulations in the design of controlled drug delivery mechanisms, such as thermal,[3] magnetic,[4] and electrical modalities.[5] Intrinsic electric fields within human physiology are crucial for modulating biological functions and eliciting action potentials in neural and muscular systems.[6–8] Electric pulses emanating from electrodes have been shown to enhance both molecular release and permeation in these systems.[9–12] However, the current dependence on wired and battery-powered electrodes impedes precise spatial electrical stimulation.[13,14]

a Department of Prosthodontics, Shanghai Ninth People's Hospital, Shanghai Jiao Tong University, School of Medicine, College of Stomatology, Shanghai Jiao Tong University, National Center for Stomatology, National Clinical Research Center for Oral Diseases, Shanghai Key Laboratory of Stomatology, Shanghai Research Institute of Stomatology, No. 639 Zhizaoju Road, Shanghai 200011, China. E-mail: xinquanjiang@aliyun.com, echomet@126.com
b State Key Laboratory of Metastable Materials Science and Technology, Nanobiotechnology Key Lab of Hebei Province, Applying Chemistry Key Lab of Hebei Province, Yanshan University, Qinhuangdao, 066004, China
† These authors contributed equally to this work.

The piezoelectric effect refers to the phenomenon where specific materials generate an electrical charge upon experiencing mechanical stress. This occurrence is attributed to the polarization of molecules within the material structure, leading to the emergence of an electrical potential. Conversely, these piezoelectric materials also exhibit the capability to undergo mechanical deformation when subjected to an electrical current, illustrating the bidirectional nature of this effect. Fundamentally, the piezoelectric effect represents a transduction mechanism, converting mechanical energy into electrical energy and *vice versa*, thus bridging the domains of mechanical and electrical phenomena.[15,16]
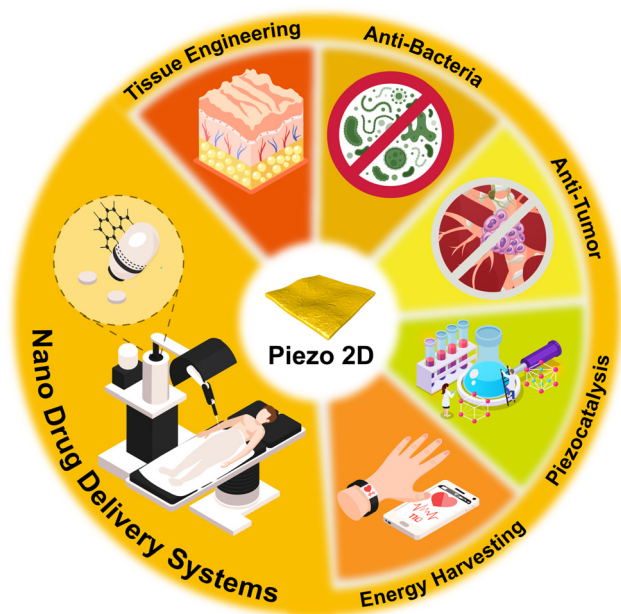
Piezoelectric materials have been widely applied in energy sources,[17] actuation,[18,19] sensing,[14,18,20,21] environmental protection,[22] and catalysis.[23,24] With the verification of their biocompatibility, piezoelectric materials have attracted considerable attention in biomedical applications.[25] Usually, some drugs need to be transferred to specific tissues/organs, including brain tissues and concealed tumors.[26–29] Compared with wearable or implantable bulk piezoelectric materials, nanoscale piezoelectric materials can be precisely delivered to the targeted tissue *via* the circulatory system.[29] Piezoelectric nanomaterials can be remotely activated by external mechanical stress (*e.g.*, ultrasound) to produce electrical charges *in situ* and achieve noninvasive drug release with better spatial resolution.[16,30–32]

Among piezoelectric nanomaterials, two-dimensional (2D) nanosheets mimic natural membranes[33] and enhance the bionano

Scheme 1 New evidence for piezoelectric nanomaterials across energy harvesting, piezocatalysis, and biomedicine fields, guiding and supporting future drug delivery system development.

interactions between the nanosheet surface and biosurface,[34] including proteins and cells.[35] 2D nanosheets, sheet-like planar shapes under weak van der Waals forces, have sparked great potential in biomedical engineering due to their distinctive optical,[36] electrical,[37] and mechanical characteristics.[38–40] The high surface-to-volume ratio of 2D nanosheets enables the loading of various therapeutic payloads *via* noncovalent interactions.[41–43] Moreover, the high surface energy of 2D nanosheets with surface and edge defects offers an essential active site for surface functionalization.[44–47] The increased surface tunability allows the construction of targeted drug delivery systems.[48]

Recent research has also reported the advanced properties of piezoelectric 2D nanosheets in the energy and catalysis fields.[49–51] Although these properties meet the demands of drug delivery systems, there is a time lag in the discussion, design, and fabrication due to the gap between different fields. The remotely controlled drug delivery system with spatial-temporal precision has theoretical significance and practical value for future medication.[52–54] Thus, this paper offers potential pursued research ideas and directions in the future for drug delivery system fabrication and disease treatment using piezoelectric materials based on previous studies (Scheme 1). This paper also intends to provide a foundation and guidelines for drug delivery system investigation and development.

2 Piezoelectricity of representative 2D materials

Piezoelectric bulk materials show promise in transducers for human–machine interfaces[55] and electroactive scaffolds for tissue regeneration.[56,57] Conversely, nanoscale piezoelectric materials excel in targeting specific body sites and penetrating cytomembranes to create internal electrical fields crucial for cell fate determination.[16] Notably, 2D nanosheets, characterized by higher piezoelectric coefficients and greater surface-to-volume ratios,[58] fall into three categories: 'flattened' bulk materials, 'stripped' asymmetrical monolayers from symmetrical bulk materials, and 'decorated' symmetrical 2D nanosheets with interfacial polar symmetry.[59] Additionally, piezoelectric bioactive molecules, including amino acids, peptides, and proteins, have potential in developing engineered healthcare materials.

2.1 Traditional piezoelectric 2D materials

In the realm of conventional bulk piezoelectric materials, these materials are primarily classified into two categories: piezoelectric polymers and ceramics. Among piezoelectric polymers, notable examples include polyvinylidene fluoride (PVDF), poly(vinylidene fluoride-trifluoroethylene) (P(VDF-TrFE)), and polyvinyl chloride. Conversely, barium titanate ($BaTiO_3$) and zinc oxide (ZnO) stand out as quintessential piezoelectric ceramics. PVDF is distinguished by its exceptional flexibility, straightforward processing methodology, and satisfactory biocompatibility. This polymer is characterized by its ability to exist in five distinct crystalline phase configurations, namely, α, β, γ, δ, and ε, with the α- and β-phases being the most significant. The α-phase of PVDF, owing to the reverse parallel arrangement of its dipoles, exhibits minimal piezoelectricity. However, during the electrospinning process, PVDF undergoes mechanical stretching coupled with *in situ* poling, resulting in a transformation of the nonpolar α-phase into a highly polar β-phase.[60] The parallel-arranged dipoles in β-phase PVDF result in a strong dipole moment per unit cell and enhanced piezoelectric characteristics.[61]

Nanopillar morphologies are achievable on PVDF film surfaces,[62] yet 2D nanosheets of PVDF and other piezoelectric polymers remain undeveloped, likely due to viscoelastic difference-induced interfacial instabilities in PVDF nanofibers.[63] Nevertheless, P(VDF-TrFE) nanotubes and spheres are fabricable.[16] Advancements in nanoscale piezoelectric polymers, particularly through the Langmuir–Blodgett technique, have yielded ultrathin P(VDF-TrFE) films with a minimum average thickness of 2.072 nm.[64] This nanoscale innovation is set to enhance piezoelectric polymers' applications in precision medicine, spanning scaffolds to drug delivery systems and pharmaceuticals.

Piezoelectric materials ideally require high electromechanical (k_{33}) and piezoelectric (d_{33}) coefficients. Yet, piezoelectric polymers often have lower k_{33} and d_{33} values compared to commonly used ferroelectric ceramics and crystals like $Pb(ZrTi)O_3$.[65] Interestingly, certain inorganic ceramics, such as hexagonal cadmium sulfide and ZnO, maintain piezoelectric properties even when reduced to nanoscale thicknesses. Specifically, 2D nanosheets of cadmium sulfide and ZnO show enhanced vertical d_{33} compared to their bulk counterparts, likely due to reduced carrier concentration and altered local polarization.[16] Additionally, the piezoelectric efficiency of synthesized ZnO has been confirmed, revealing structure-dependent performance, with higher surface-to-volume ratio structures exhibiting superior efficacy.

For polymer–ceramic composites, a $Ti_3C_2T_x$ MXene anchoring method has been recently proposed to manipulate the

intermolecular interactions within the all-*trans* conformation of a polymer matrix.[66] β-Phase programming boosts the piezoelectric response of samarium-doped $Pb(Mg_{1/3}Nb_{2/3})O_3$–$PbTiO_3$/PVDF composite nanofibers by 160% *via* $Ti_3C_2T_x$ 2D nanosheet inclusion.

2.2 Monolayer and few-layer piezoelectric materials

In addition to flattened conventional piezoelectric ceramics, the piezoelectric effect has been observed in 2D nanosheets whose bulk counterparts do not possess piezoelectric properties, such as MoS_2. In 2014, Wang *et al.* first conducted an experimental study on the piezoelectric properties of MoS_2 2D nanosheets. Due to the loss of centrosymmetry, the MoS_2 2D nanosheets with an odd number of atomic layers produced piezoelectric voltage and current outputs, whereas the even number of layers showed no current. Similarly, piezoelectricity has been verified in transition metal dichalcogenides (TMDCs), such as WSe_2. Insulating monolayer hexagonal boron nitride (BN) has also been proven to have piezoelectric properties. Owing to the 2D confinement, these materials display unique electronic, optical, and mechanical properties that are unattainable in their bulk counterparts. Cheon *et al.* conducted data mining for over 50 000 inorganic crystals and predicted 325 potential piezoelectric monolayers, which significantly extends the scope of 2D piezoelectric materials.

Apart from conventional piezoelectric ceramics, 2D nanosheets like MoS_2, which lack piezoelectricity in bulk form, exhibit piezoelectric effects. Wang *et al.* in 2014 first experimentally demonstrated MoS_2 2D nanosheets' piezoelectric properties,[67] where odd-layered sheets generated piezoelectric voltage and current, unlike even-layered ones. This piezoelectricity is also present in transition metal dichalcogenides like WSe_2 and in insulating monolayer hexagonal boron nitride (BN).[68,69] These 2D materials showcase distinct electronic, optical, and mechanical properties, divergent from their bulk forms.[70] Additionally, Cheon *et al.*'s data mining of over 50 000 inorganic crystals identified 325 potential piezoelectric monolayers, broadening the range of 2D piezoelectric materials.[71]

Differing from TMDC monolayers, certain 'stripped' 2D nanosheets like graphene lack asymmetric crystalline structures and gain piezoelectric properties only when chemically modified or structurally defected to disrupt centrosymmetry.[72] Moreover, in Schottky junctions—classic interfaces between noble metals and centrosymmetric semiconductors—the built-in electric field within the depletion region can induce polar structures in the semiconductors, thereby generating piezoelectric effects.[59]

2.3 Bioactive piezoelectric 2D materials

Inside the human body, the principle of piezoelectricity relies on numerous biological counterparts, from basic building blocks, including amino acids and proteins, to highly organized tissues, such as skin, muscle and bone.[73]

Amino acids. Amino acids, basic organic compounds, contain a carboxyl (–COOH) group, an amine (–NH_2) group, hydrogen, and a specific side functional group (R). Most of them exhibit chirality and thus piezoelectricity. Glycine, unique as a nonchiral amino acid with hydrogen as its side group, crystallizes

into α, β, and γ polymorphs. α-Glycine's central symmetry precludes piezoelectricity, whereas β- and γ-glycine's asymmetry confers it.[74] Self-assembled glycine 2D nanosheets, created *via* spin-coating, demonstrate piezoelectricity, a high nonlinear optical coefficient, wide transparency, and high damage threshold in β-glycine.[75] An applied force of 0.172 N on these nanosheets yields an open-circuit voltage of 0.45 V. The potential for assembling amino acids into peptides and proteins through dehydration condensation opens avenues for fabricating biological piezoelectric materials.

Peptides and proteins. Short peptides, created by amino acid linkage, can exhibit piezoelectric properties. Notably, diphenylalanine, a dipeptide of two phenylalanine molecules, stands out as a significant piezoelectric biomolecule. Kholkin *et al.* synthesized diphenylalanine 2D nanosheets, nanotubes, and nanofibers through solution processes, confirming their piezoelectricity *via* piezoresponse force microscopy.[76] The synthetic polypeptide poly-γ-benzyl-L-glutamate, with an α-helical structure, has demonstrated a piezoelectric coefficient (d_{14}) of 26 pC N^{-1} when oriented in a magnetic field.[77]

Extracellular matrix bioactive proteins like collagen, fibrin, and keratin exhibit piezoelectricity, influencing cellular activity regulation. Collagen's piezoelectric properties are sensitive to pH and humidity, which can alter its polar bond activity and crystalline structure,[78] leading to varied piezoelectric characteristics based on processing. Emulating biological piezoelectricity, Yang *et al.* produced an ultrathin collagen fibril nanofilm using small intestinal submucosa through van der Waals exfoliation,[79] although its size isn't customizable. Vivekananthan *et al.* pioneered a collagen film-based piezoelectric energy generator.[80] This device, created by sandwiching a collagen film between two conducting films and laminating with polypropylene, outperforms traditional ceramic/oxide humidity sensors. It' is a self-powered, non-toxic, eco-friendly piezoelectric biopolymer with notable sensitivity and reliability. Under a 5 N force, it generates a maximum V_{oc} of 50 V and I_{sc} of 250 nA. As a humidity sensor, it demonstrates linear responsiveness between 50 and 90% relative humidity, with a sensitivity of 0.1287 μA $\%^{-1}$ relative humidity.

The challenge of arranging ordered piezoelectric domains has hindered the creation of uniformly distributed piezoelectric 2D nanosheets through natural collagen assembly. However, given their biocompatibility and degradability, bioactive molecule-synthesized piezoelectric 2D nanosheets hold potential in regenerative medicine. Beyond intrinsic piezoelectric properties, Takano *et al.* discovered a piezoelectric-like effect in myosin *via* molecular dynamics simulation.[81] Mechanical stimuli applied locally on proteins can trigger electrostatic potential changes in remote areas, a process termed piezoelectric allostery. This input/output mechanism implies that mechanical input at a specific site can cause extensive structural changes in proteins, resulting in altered electrostatic potential. Such dynamic transduction could lead to the design of protein-based biomaterials.

2.4 Biocompatibility of piezoelectric 2D materials

Biocompatibility refers to the compatibility of materials with biological systems, particularly focusing on adverse biological

reactions and stability within organisms.[82] A material with high biocompatibility does not trigger immune responses, inflammation, or other harmful reactions, while maintaining its functionality and performance within the biological environment. Biocompatibility encompasses compatibility with cells, blood, and tissues, and also considers the material's genotoxicity and neurotoxicity.[83] Exceptional biocompatibility is a critical prerequisite for clinical applications of all biomaterials.

Lead-based piezoelectric ceramics, such as lead zirconate titanate, despite their excellent electrical properties, are excluded from biomedical applications due to their widespread biotoxicity, especially in the development of drug delivery systems.[84] In contrast, lead-free piezoelectric ceramics like $BaTiO_3$ demonstrate superior biocompatibility, making them more suitable for biomedical purposes.[85] Additionally, ZnO piezoelectric 2D materials not only circumvent the toxicity issues associated with lead-containing materials but also exhibit properties that enhance cell proliferation.[86]

Monolayer or few-layer 2D nanomaterials exhibit notable biocompatibility. For instance, 2D BN nanomaterials with graphene-like structures have demonstrated exceptional biocompatibility in both *in vitro* and *in vivo* studies. This is primarily attributed to their propensity to adsorb onto cell membrane surfaces without penetrating the cells.[87] However, as the size of BN increases to the micrometer scale, its biotoxicity significantly escalates.[88] Another category of 2D materials, piezoelectric TMDCs, such as MoS_2,[89] WS_2,[90] and TiS_2,[91] are also widely used in the field of biomaterials and have been confirmed to possess good compatibility with cells, blood, and tissues. Under physiological conditions, unmodified 2D TMDCs face challenges in direct application in drug delivery systems due to inadequate colloidal stability.[92] Consequently, combining these piezoelectric 2D nanomaterials with organic coatings to enhance their solubility, dispersibility, and stability can facilitate their acceptance by biological systems. It is important to note that while these piezoelectric 2D nanomaterials do not inherently elicit adverse biological reactions, their interaction with aquatic perfluoroalkyl substances, such as MoS_2 and WS_2, can lead to significant accumulation in zebrafish, causing oxidative stress in the liver and intestines.[93] The biotoxicity arising from such interactions between toxic substances and nanomedicines is a critical concern in the biological application of piezoelectric 2D nanomaterials.

Natural piezoelectric materials (like amino acids, peptides, and proteins) are generally considered biologically safe. However, apart from amino acids and shorter peptides, the unique three-dimensional structures and surface characteristics of longer peptides[94] or proteins[95] can act as antigenic determinants, triggering recognition and activation by the immune system. Therefore, the antigenicity of naturally derived piezoelectric materials should be a key consideration when selecting them for internal applications. Despite potential antigenicity concerns, bio-derived piezoelectric nanomaterials demonstrate exceptional *in vivo* degradability. These natural materials decompose into fundamental molecules like water and carbon dioxide under physiological conditions, or are reabsorbed by the body.[96] For instance, glycine, a piezoelectric amino acid, is

absorbed in the small intestine and breaks down into ammonia and carbon dioxide under the action of the glycine cleavage system enzyme.[97] Collagen fibers, another piezoelectric material, exhibit variable degradation times based on their degree of crosslinking. In Sprague-Dawley rats, non-crosslinked collagen scaffolds degrade rapidly within three weeks, whereas those treated with glutaraldehyde maintain structural integrity for up to nine weeks.[98] This characteristic is crucial for certain implantable piezoelectric devices, allowing the adjustment of expected degradation times to align with treatment periods, thereby minimizing the trauma associated with secondary surgeries required for device removal.

3 Piezocatalysis-related biomedical uses of piezoelectric 2D nanosheets

Piezoelectric 2D nanosheets are suggested to facilitate redox reactions in catalysis, generating oxidants, antioxidants and gas molecules that have effects on biomedical applications.

3.1 Mechanisms of piezocatalysis

Piezoelectric material catalysis fundamentally involves dipole orientation shifts, leading to bound charge changes. Stress-induced dipole alterations in the catalyst disrupt local free charge concentration, initiating redox reactions.[23,99] Piezoelectric 2D nanosheets, with their ultrathin structure, reduce the energy barrier by shortening the charge carrier transport distance (for electrons and holes), thereby enhancing reactant adsorption and activation. These nanosheets are adept at fostering specific reactions while suppressing competing ones, thereby controlling catalytic reaction efficiency and selectivity.[100] For instance, Fig. 1(a) illustrates single-layer MoS_2 decomposing water to generate reactive oxygen species *via* spontaneous polarization and catalysis, whereas Fig. 1(b) depicts the decomposition of rhodamine B dye through this mechanism.[24]

Defect engineering shapes the physicochemical properties of catalysts, enhancing catalysis through atomic rearrangement, charge redistribution, energy band changes, and optimization of intermediate adsorption–desorption and charge/mass transfer.[24] This approach has been widely applied in piezocatalysis and cocatalysis.[101,102] Combining piezoelectric output with piezocatalysis, piezo-photocatalysis, piezotronics, and piezophototronics has led to advancements in sensing and pollutant degradation,[103–105] leveraging the established piezoelectric effect of 2D nanosheets. These nanosheets also show promise in biomedical applications, such as using ultrasound-driven piezocatalytic bismuth oxychloride 2D nanosheets for disintegrating Alzheimer's β-amyloid aggregates into harmless fragments,[106] and in antitumor and antibacterial therapies.[107,108] Therefore, the exploration and application of catalytic piezoelectric 2D nanosheets can significantly contribute to biomedical solutions through chemical reactions, a potential often overlooked by researchers.

3.2 Products generated *via* piezocatalysis

Piezoelectric 2D nanosheets are revolutionizing green catalysis by converting mechanical energy, particularly in water's
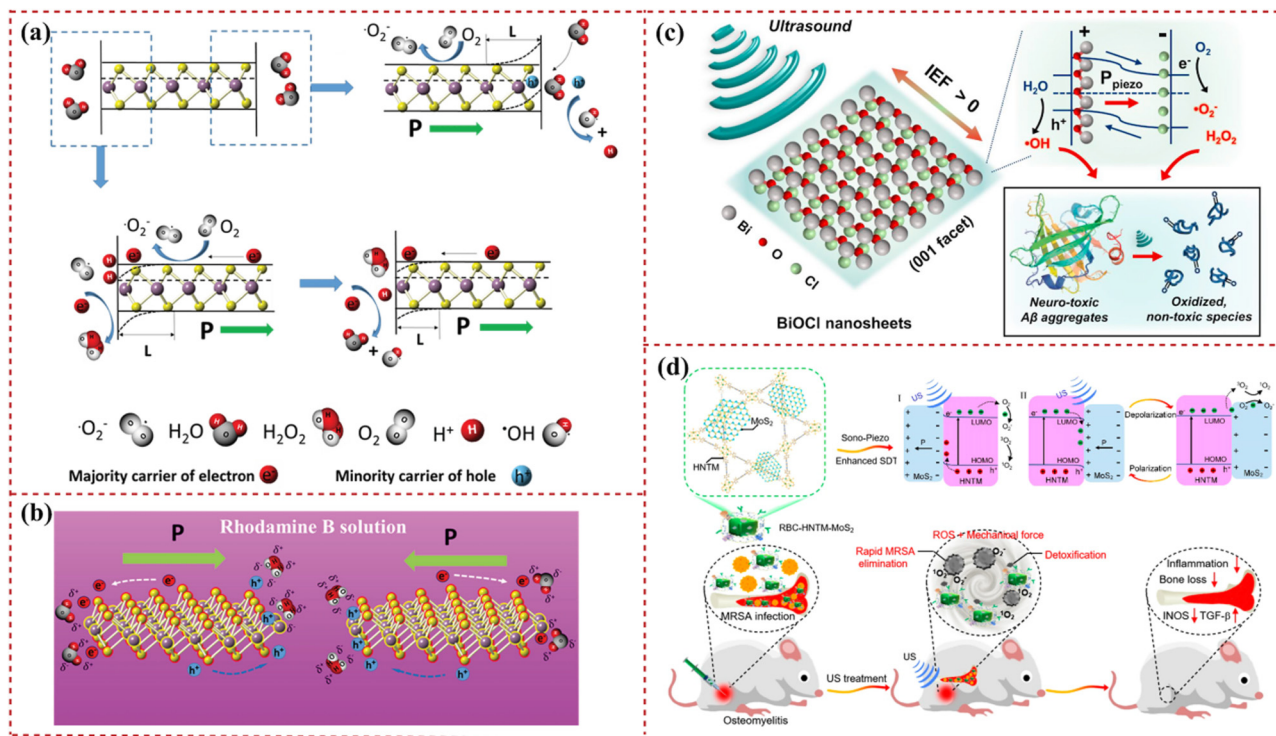
Fig. 1 Schematic illustration of the catalytic effect of piezoelectric 2D nanosheets. (a) Working principle of the degradation activity through the piezocatalytic effect of single-layer MoS$_2$. (b) The reduction and oxidation process of single-layer MoS$_2$ for destroying the organic dye by spatially spontaneous polarization and the catalyzing process. Reprinted with permission from ref. 24. Copyright 2016, Wiley-VCH Verlag GmbH & Co. KGaA, Weinheim. (c) Illustration of piezoelectric dissociation of Alzheimer's β-amyloid (Aβ) aggregates on a bismuth oxychloride 2D nanosheet surface (IEF: internal electric field). Reprinted with permission from ref. 106. Copyright 2020, Elsevier B.V. (d) Sonocatalytic mechanism of hollow metal–organic framework-MoS$_2$ and efficient sonodynamic therapy treatment of osteomyelitis through rapid bacterial elimination and detoxification. Reprinted with permission from ref. 109. Copyright 2022 American Chemical Society.

hydrogen and oxygen evolution processes.[110,111] Hydrogen, notably promising in tissue regeneration,[112] serves as a therapeutic agent in ischemic tissue injury recovery and metabolic syndrome management.[113–115] It mitigates bone loss by reducing oxidative stress and TNFα-induced damage in osteoblasts[116,117] and lessens steroid-associated femoral head necrosis in rabbits through hydrogen-rich saline.[118] Furthermore, hydrogen's role in diminishing neuroinflammation, closely linked to oxidative stress, is notable.[119,120] In early brain injury scenarios, hydrogen protects against oxidative stress-induced damage by influencing gene transcription and controlling the generation of oxidized phospholipids.

Molecular hydrogen's extensive medical applications necessitate designing carriers for its storage and controlled release. While hydrogen is generally non-toxic, its systemic administration can cause minor side effects like heartburn, diarrhea, and headaches.[121] Nanoscale hydrogen delivery systems offer precise microenvironment regulation, proving effective in treating Alzheimer's disease,[122] fatty liver disease,[123] diabetic feet,[124] and exercise-induced inflammation.[125] Interestingly, carbon monoxide (CO) and reactive oxygen species (ROS), typically deemed toxic, are byproducts of piezocatalysis. Their targeted, controlled release can yield therapeutic effects in specific tissues while minimizing systemic toxicity, applicable in tumor treatment,[126] anti-infective therapy, and cardiovascular and nervous system protection.[127,128] The 2D structure,

with its large surface-to-volume ratio, is particularly suited for hydrogen generation and anti-inflammatory therapy.[129] Piezocatalytic nanoparticles enhance hydrogen generation rates and enable targeted release within the human body (Scheme 2).

3.3 Piezocatalysis-related neurodegenerative disease treatment

Piezocatalysis can be a potential treatment for Alzheimer's disease (AD). Research indicates that self-assembly, accumulation, and deposition of Aβ aggregates in the central nervous system are key AD pathologies.[106,130] 2D nanosheets are effective in absorbing amyloid peptides, impeding conformational transitions and fibrillation, thus decelerating disease progression.[131] Park et al. developed an ultrasound-driven piezocatalytic platform using BiOCl 2D nanosheets, which successfully broke down Aβ aggregates into non-toxic fragments (Fig. 1(c)).[106] Ex vivo studies showed a significant reduction in Aβ plaque density in AD mouse brain slices from 121.6 cm^{-2} to 25.2 cm^{-2} using sono-activated BiOCl 2D nanosheets. These nanosheets are believed to disrupt Aβ aggregates' strong side-chain interactions through piezocatalytic redox reactions.

3.4 Piezocatalysis-related antibacterial treatment

Bone defects infected by *Staphylococcus aureus* can lead to complications like osteomyelitis, impeding bone regeneration
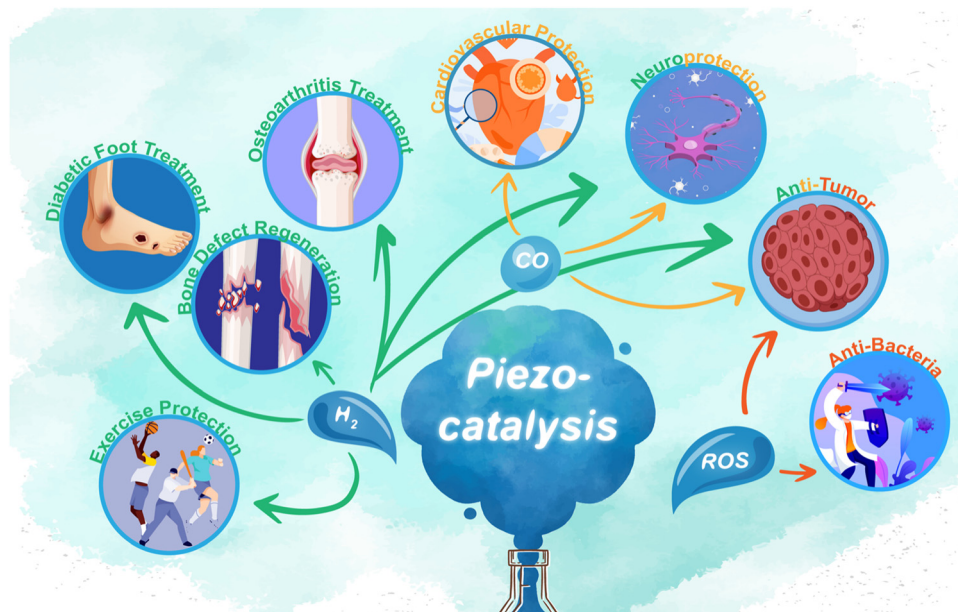
Scheme 2 Schematic diagram of the applications of piezocatalysis products H_2, CO, and ROS in the field of biomedical science.

and causing secondary bone loss.[132] Piezoelectric 2D MoS_2 nanosheets have been shown to promote osteogenesis by reducing bone loss through infection and inflammation inhibition. These nanosheets are proven to induce bone integration and demonstrate good biocompatibility.[133] The ROS generated *via* piezocatalysis can efficiently kill methicillin-resistant *Staphylococcus aureus* within 20 min under ultrasonic excitation, as illustrated in Fig. 1(d). The red blood cell membrane-coated MoS_2 reduces inflammation and suppresses bone destruction, evidenced by a decrease in bone defect area after effective sonodynamic treatment. Consequently, piezoelectric MoS_2 2D nanosheets are significant in treating bacterium-infected osteomyelitis, substantially reducing inflammation and bone loss.[108,134]

3.5 Piezocatalysis-related tumor therapy

Due to the acoustic excitation properties of piezoelectric catalysis, it facilitates remote stimulation for *in situ* controllable catalytic therapy within the body. Combined with the dimensional characteristics of piezoelectric two-dimensional nanosheets, localized catalytic treatment of tumors becomes feasible. A strategic piezoelectric-mediated drug delivery system is designed to downregulate tumor interstitial fluid pressure *via* water splitting of MoS_2 in the tumor interstitium, which employs piezocatalysis to downregulate tumor interstitial fluid pressure and enhance intratumoral drug delivery. Piezocatalytic therapy has been demonstrated as a potential universal strategy for promoting intratumoral drug delivery, eliminating deep tumor cells, and inhibiting tumor recurrence by Gao *et al.* (Fig. 2(a)).[135] In addition, piezocatalysis can be applied to activate tumor immunotherapy. He *et al.* have discussed a novel approach for treating deep tumors using ultrasound-driven piezocatalysis. The method utilizes a piezoelectric 2D nanosheet to produce hydrogen molecules and reduce lactic acid under ultrasonic stimulation. This process

effectively inhibits liver tumor growth through immune regulation of the tumor microenvironment. Piezocatalytic hydrogen generation is highly responsive to ultrasound irradiation, allowing for controlled catalytic reactions and on-demand therapy (Fig. 2(b)).[136]

4 Electrical signal-related biomedical uses of piezoelectric 2D nanosheets

Piezoelectric nanomaterials, including pyroelectric and ferroelectric materials,[137] offer mechanical and electrical stimuli for tissue regeneration,[10,43,138] capable of converting various energy types such as force, heat, electricity, and light into electrical, mechanical, and optical signals. These conversions can harness energy changes within tissue microenvironments. When integrated into scaffolds, piezoelectric nanomaterials can generate electrical signals to induce tissue regeneration, mimicking pathways in the extracellular matrix.[139] Ultrathin 2D nanosheets, a type of piezoelectric nanomaterial, feature a high surface-to-volume ratio, significant anisotropy, and superior chemical and mechanical properties.[140] Their unique morphology fosters special 'nano-bio' interactions, affecting biological activities like intracellular trafficking, biodistribution, and biodegradation. The ultrathin structure also offers advantageous transport and physicochemical properties for energy and catalytic applications.[16] Additionally, these nanomaterials can function as targeted drugs, endocytosed into cells to create intracellular electrical fields. Current biomedical applications of piezoelectric 2D nanomaterials are detailed in Table 1, indicating a prospective trajectory for future biomedical strategies involving these materials.

4.1 Bone repair and regeneration

Piezoelectricity in natural bone. It has been reported that piezoelectricity is essential in regulating natural bone
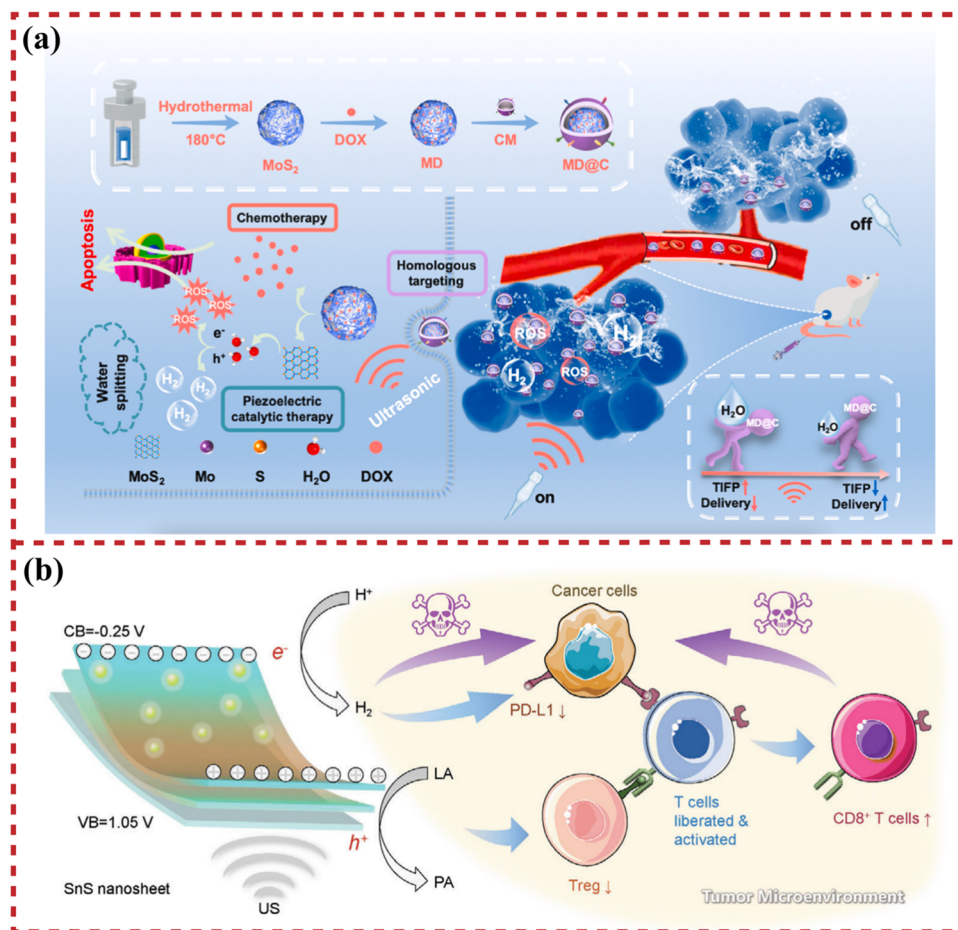
Fig. 2 The applications of piezoelectric 2D nanosheets in piezocatalysis–related tumor therapy. (a) Schematic illustration of the construction procedure of the MoS$_2$·DOX@cytomembrane (MD@C) and the mechanism of piezocatalytic enhancement of penetration ability in solid tumors. Reprinted with permission from ref. 135. Copyright 2022, Elsevier B.V. (b) Schematic illustration of the mechanism of SnS nanosheet–mediated piezocatalytic hydrogen generation and lactic acid deprivation for tumor immunoactivation. Reprinted with permission from ref. 136. Copyright 2023, Wiley-VCH Verlag GmbH & Co. KGaA, Weinheim.

metabolic activities, such as bone growth, structural remodelling and fracture healing. Halperin *et al.* found that the variation in d_{33} ranges from 7.7–8.7 pC N^{-1} for the human tibia.[108] The asymmetric structure of collagen molecules leads to the piezoelectricity of natural bone.[78] The collagen molecule is made from three polypeptide strands connected *via* hydrogen bonds and twisted to form a triple helix structure. It can generate piezoelectricity by changing the orientation of dipoles of –NH and –CO groups. Under mechanical stress, collagen fibres undergo various motions, such as rotation and sliding, leading to the generation of electrical charges. The broken hexagonal symmetry of their structure at the nanometric level is what causes the piezoelectric action. Additionally, ion motions in the mineralized matrix control the production of electrical potentials in the bone under mechanical stress.[155,156]

The piezoelectricity of collagen fibres, the key component of the bone tissue extracellular matrix, stimulates various cellular activities within the bone microenvironment. Compressive loads increase the negative charge on collagen fibres in the periosteum, thus facilitating osteoblast perception of electrical cues.[157,158] The voltage-gated calcium channels on the cytomembrane open under the effect of electrical signals, resulting in a Ca^{2+} influx into the cytoplasm. The signaling pathways triggered by Ca^{2+} ultimately activate R_{as} and the extracellular signal-related protein kinase signaling pathway, which is critical for Runx2 activation and the induction of several growth factors, such as TGF-β and BMP.[159]

Osteogenic piezoelectric 2D nanosheets

ZnO. ZnO crystals, featuring three rapid growth directions, enable a range of morphologies from 0D to 3D.[160] Their nanomaterials, synthesized through various crystal-growth techniques, exhibit notable semiconductivity, piezoelectricity, chemical stability, and biocompatibility.[108,161] Bone tissue generates electrical stimulation in response to mechanical stress, a process reflecting the piezoelectric materials' ability to harvest and redistribute energy, thus countering energy entropy increase. This mechanical energy is partially converted into electricity through piezoelectricity to regulate cellular activities. Esteve *et al.* demonstrated this by culturing osteoblast-like cells (Saos-2) on piezoelectric ZnO 2D nanosheets,[141] as depicted in

Table 1 2D piezoelectric nanomaterials for biomedical uses

Nanostructured material	Length (L)/diameter (D)/thickness (T)	Synthesis method	Piezoelectric strain coefficient	Applied load/ultrasonic intensity	Output voltage	Output current	Application	Animal model	Ref.
ZnO nanosheets	$D \approx$ 1–2 μm $T \approx$ 20 nm	Hydrothermal method	d_{33} = 4–6 pC N^{-1}	0.65 N	0.5–50 mV	—	Osteogenic differentiation of cells	—	141
GaN/AlGaN heterostructures	$T \approx$ 50 nm	Metal–organic chemical vapour deposition	—	—	0.311 mV	—	Promotion of bone regeneration	Rat distal femur defect	142
Hierarchical PVDF/ZIF-8	$D \approx$ 500 nm	solid-state shear milling, salt leaching method	d_{33} = 3.5 pC N^{-1}	—	10 V	—	Vascularized bone regeneration	Critical size calvarial defect model in rats and femoral defect model in mice	143
MoS$_2$ nanosheets	$D \approx$ 20 nm	Hydrothermal method	—	1.5 W cm^{-2}, 50% duty cycle, 1 MHz	—	0.15 μA cm^{-2}	Control of osteomyelitis and promotion of bone formation	Rat osteomyelitis model	109
BN nanosheets	$D \approx$ 1.3 μm	Electrospinning technique, oleylamine-assisted exfoliation method	—	Sound pressure of 80–110 dB at a fixed frequency of 1 kHz	10–15 V	—	Promotion of bone regeneration	—	144
Black phosphorus nanosheets	D = 300–500 nm	Liquid exfoliating method	—	1.5 W cm^{-2}, 50% duty cycle, 1 MHz	—	—	Anti-infection and improved bone-implant integration	Rat infection and bone-implant integration	145
CaO$_2$-loaded titanium carbide nanosheets	T = 2–3 nm	Facile exfoliation and intercalation method	—	1 W cm^{-2}, 50% duty cycle, 1 MHz	—	—	Anti-infection and promotion of bone regeneration	Wound healing model and prosthetic joint infection model in rats	146
Nb$_2$C nanosheets	$D \approx$ 2 μm	Hydrothermal method	—	1.5 W cm^{-2}, 50% duty cycle, 1 MHz	—	—	Anti-infection and promotion of bone regeneration	Rat infected bone defect model	147
Ti$_3$C$_2$ nanosheets	T = 50 nm	Chemical exfoliation method	—	1.5 W cm^{-2}, 50% duty cycle, 1 MHz	—	0.02 μA cm^{-2}	Anti-infection	Mouse bony tissue infection model	148
WS$_2$ nanosheets	$D \approx$ 100 nm $T \approx$ 5.5 nm	Hydrothermal method	d_{11} = 2.12–3.23 pC N^{-1}	0.5 W cm^{-2}, 2 min, 1 MHz	—	—	Tumor treatment	MCF-7 tumor-bearing mice	149
MoS$_2$ nanosheets	$D \approx$ 300 nm	Lithium intercalation method	—	1 W/cm^2, 50% duty cycle, 1 MHz	0.02 V	—	Piezocatalysis of tumor treatment	4T1 tumor-bearing mouse model	150
Graphene oxide-TiO$_2$–MnO$_x$ nanosheets	$D \approx$ 230 nm	Seeded growth method	—	1 W cm^{-2}, 50% duty cycle, 60 sec, 1 MHz	2.1 V	—	Piezocatalysis of tumor treatment	4T1 tumor-bearing mouse model	151
FePS$_3$ nanosheets	T = 4 nm	Ultrasound-assisted liquid phase exfoliation method	—	0.5 W cm^{-2}, 50% duty cycle, 1 MHz	—	—	Chemodynamic/sonodynamic catalysis of tumor treatment	4T1 tumor-bearing mouse model	152

Table 1 (*continued*)

Nanostructured material	Length (L)/diameter (D)/thickness (T)	Synthesis method	Piezoelectric strain coefficient	Applied load/ultrasonic intensity	Output voltage	Output current	Application	Animal model	Ref.
MoS$_2$ nanoflowers	$D \approx 100$ nm	Hydrothermal method	—	1.5 W cm^{-2}, 50% duty cycle, 1 MHz	—	0.01 μA	Piezocatalysis of water decomposition to reduce tumor pressure	U14 tumor-bearing mouse model	135
2D niobate-lead titanate piezo-array	$L \approx 10$ mm	Dicing-and-filling method	$d_{33} = 1200$ pC N^{-1}	3.3-MHz ultrasonic pulse	—	—	Piezoelectricity-induced retinal stimulation	—	153
ZnO nanosheets	$D \approx 87$ nm	Chemical bath deposition method	—	—	—	—	Nerve agent detection	—	154
BiOCl nanosheets	$D = 0.8$–2.5 μm $T = 200$–470 nm	Hydrothermal method	—	70 W, 40 kHz, 24 h	—	—	Piezocatalysis of protein structure decomposition	Alzheimer's disease mouse model	106
SnS nanosheets	$L \approx 150$ nm $T = 0.8$ nm	Solvothermal method	—	2–3 W cm^{-2}, 10% duty cycle, 40 kHz	—	—	Piezocatalysis for intra-tumoral immune activation	Hepa 1-6-Luc cells tumor-bearing mouse model	136

Fig. 3(b). The nanosheets' reduced thickness (around 20 nm) and high aspect ratio enable deflection from inherent cell forces without external stimulation. These minute cell forces, in the nanonewton range, generate a piezoelectric potential of 0.5–50 mV, activating voltage-gated and stretch-activated calcium channels. Consequently, this leads to elevated expression of osteoblast differentiation genes.

Cell movement strains ZnO 2D nanosheets, producing local electric fields through piezoelectricity. These fields open voltage-gated calcium channels, enhancing cell proliferation and early differentiation. Furthermore, when used as drug nanocarriers, the electric signals from cell–nanosheet interactions can synergize with drug internalization.[162] The applied electric field also influences cell alignment and migration, known as electrotaxis—the directed cell movement in response to electric cues.[163] This property is advantageous for targeted drug delivery.

BN. When considering piezoelectricity, BN nanotube hybrid piezoelectric scaffolds show enhanced proliferation and osteogenic differentiation of MC3T3-E1 cells and Saos-2 cells.[164,165] Although the form of the nanotube is not quite the same as that of the 2D nanosheet, the piezoelectricity of BN can be further applied in bone tissue engineering.

MXene. MXenes ($M_{n+1}X_nT_x$, $n = 1$–3), graphene-like transition metal carbides and nitrides, are established as highly oriented piezoelectric materials.[166,167] Their surface functional groups disrupt inversion symmetry in lattice structures, endowing them with piezoelectric properties. When integrated into polymer-based scaffolds, these piezoelectric MXenes enhance the piezoelectric response.[66]

The role of MXenes (*i.e.*, Ti$_3$C$_2$T$_x$) in bone tissue engineering has been explored[168–170] and can be used as an auxiliary additive to functionalize bone regeneration scaffolds.[10,170,171] MXene-loaded scaffolds show a positive effect on spontaneous osteogenic differentiation of MC3T3-E1 preosteoblasts by accelerating the absorption of Ca^{2+}.[170] The programmable functionalization of Ti$_3$C$_2$T$_x$ MXenes endows them with stimuli-responsiveness, such as pH-responsiveness and chiral biorecognition of certain enzymes. This characteristic helps to recognize and activate MXene nanosheets in complex microenvironments, indicating their potential in targeted therapeutic nanomaterial fabrication and drug delivery systems.[172,173] However, the applications of piezoelectric MXenes are limited in bone tissue engineering thus far, which seems to be a feasible idea for future material design.

4.2 Nerve repair and regeneration

Electrical signals in neuron growth. Electric fields significantly influence neurite outgrowth and nerve tissue regeneration, paralleling osteogenesis effects.[174,175] Jaffe and Poo initially demonstrated electric fields' positive impact on neuritic growth.[176] They observed increased neuritic outgrowth in embryonic chick dorsal root ganglia cultured on polylysine-coated glass under 70–140 mV mm^{-1} electric fields. This growth is hypothesized to occur as neurite growth cones react
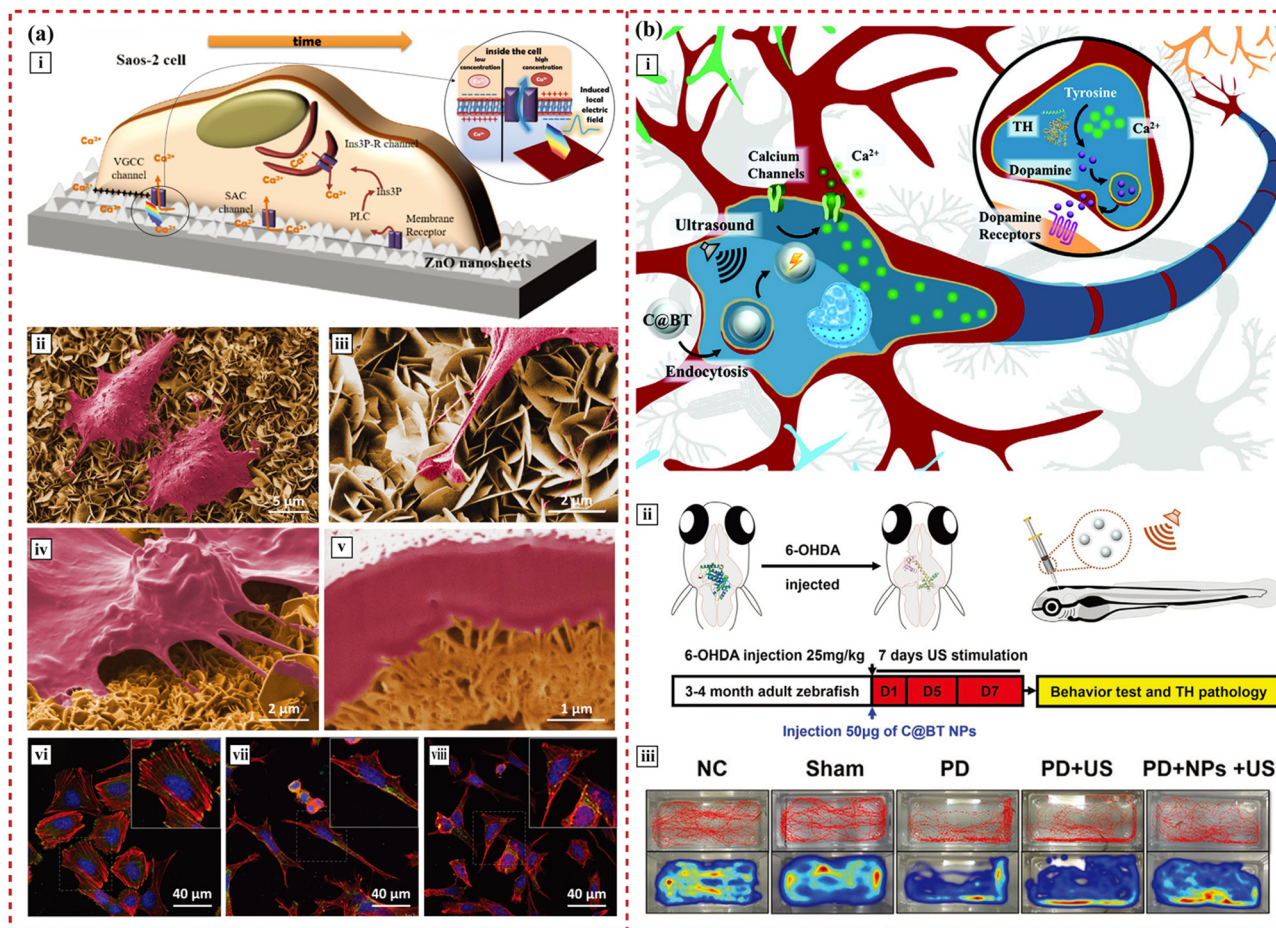
Fig. 3 The applications of piezoelectric 2D nanosheets in bone and nerve tissue engineering. (a) Self-powered piezoelectric nanogenerators based on a ZnO 2D nanosheet network. (i) Sketch of a cell growing on the top array of ZnO 2D nanosheets, indicating the possible pathways involved in cytosolic Ca^{2+} concentration changes in the osteoblast-like cells. (ii)–(v) The nanogenerator–cell interaction that is assessed by scanning electron microscopy and focused ion beam shows the firm adhesion of osteoblast-like cells on the 2D nanosheets and the emitted long projections that anchored on the 2D nanosheets. (vi)–(viii) Confocal laser scanning microscopy analysis shows a high number of focal contacts at the end of long parallel bundles of actin filaments on cells grown on AlN, displaying a polygonal shape. Reprinted with permission from ref. 141. Copyright 2017, Wiley-VCH Verlag GmbH & Co. KGaA, Weinheim. (b) Piezoelectric nanoparticles modulate neural plasticity and recovery of degenerative dopaminergic neurons. (i) The piezoelectric $BaTiO_3$ nanoparticle mediates neuron plasticity. (ii) Illustration of zebrafish injected with 6-OHDA to develop Parkinson's disease symptoms and schematic diagram of PD treatment *via* ultrasound-induced electromagnetic fields using nanoparticles. (iii) Representative spatiotemporal behavioral phenotyping in adult zebrafish under different treatments (control, sham, 6-OHDA, 6-OHDA + US, and 6-OHDA + nanoparticles + US). Reprinted with permission from ref. 194. Copyright 2020, Wiley-VCH Verlag GmbH & Co. KGaA, Weinheim.

to nerve growth factor signaling, with its receptors rearranged by electric fields. Patel and Poo further found that steady electric fields (0.1–10 V cm^{-2}) lead to pronounced neurite outgrowth towards the cathodal current and increased neuritic density, attributed to the redistribution of growth-controlling surface proteins like Concanavalin A receptors.[177]

In nerve tissue, intrinsic pulsatile electric fields create non-uniform and focal electric fields. To study neuritic outgrowth orientation in embryonic Xenopus, three types of extracellular electric fields are employed: focally applied pulsed fields, steady fields, and spatially uniform pulsed fields. While alternating currents typically induce osteogenesis, neural cell stimulation necessitates direct currents due to transmembrane potential dynamics.[178] Application of a 250 mV mm^{-1} direct electric field attracts the growth cone to negative polarities and

causes deflection towards positive polarities. Resultantly, Xenopus neurons develop longer neurites oriented towards the cathodal side and shorter neurites on the anodal side.

Electrical signal-related neurogenesis. Electrical signals are crucial not only in neural development but also in nerve repair and regeneration post-injury.[179] Injuries to the central or peripheral nervous system can impair cognitive and sensorimotor functions.[180,181] Research indicates that low-frequency pulsed electrical stimulation facilitates nerve injury regeneration.[182–184] Consequently, piezoelectric materials, which generate electrical signals under mechanical stress, can be engineered into devices for treating nerve injuries to aid nerve regeneration.

Capitalizing on the exceptional characteristics of 2D nanosheets, piezoelectric BN nanosheet-enhanced polycaprolactone channel scaffolds have been developed. BN inclusion elevates the

piezoelectric and mechanical properties of these scaffolds. It mitigates the immune response and corrects energy metabolic disturbances by lowering ROS levels. Enhanced slow-type myosin expression in the BN@polycaprolactone group indicates BN nanosheets' role in muscle structure recovery and amyotrophy reduction, likely due to microelectrical stimulation and injury area microenvironment rebalancing. This suggests concurrent regeneration of motor and sensory neurons.[185]

Piezoelectric nanomaterials in auditory nerve recovery mimic cochlear acoustic-electrical transduction by vibrating at distinct sound frequencies and conveying electrical impulses to the vestibulocochlear nerve.[182] Additionally, electroconductive 2D nanomaterials excel in differentiating mesenchymal stem cells into neural-like cells, supporting their growth.[186,187] A chip-like flexible biomimetic device, combining MXene artificial synapse with an ion-conductive elastomer, simulates the afferent nervous system.[188] This device, using piezoelectric 2D MXene layers, not only transmits external stimuli but also emulates biological neural responses like ionic migration. It converts electronic variation in ion-conductive elastomers into neuro-electric signals, detecting joint flexion and radial artery pulse. This leads to neural tissue engineering and smart medical robot design.

Li *et al.* have demonstrated neural stem cells cultured on $Ti_3C_2T_x$ MXene 2D nanosheets showed enhanced differentiation, neurite growth, and synaptic transmission.[189] $Ti_3C_2T_x$ increases voltage-gated Ca^{2+} currents in mature neurons, boosting spiking activity without altering passive membrane properties. Moreover, $Ti_3C_2T_x$ MXene interfaces maintain basal neuronal physiology, evidenced by calcium imaging and synaptic current recordings.[190]

Electrical signal-related neurodegenerative disease treatment. Neurodegenerative diseases, characterized by the progressive loss of neuronal function, prominently include Alzheimer's and Parkinson's diseases, noted for their severe complications and high prevalence.[191,192] Electromagnetic field exposure has been found to influence cell epigenetics and facilitate efficient somatic cell reprogramming, offering a potential approach for recovering degenerative neurons.[193]

Carbon-shelled $BaTiO_3$ nanoparticles, designed for endocytosis by neurons, generate intracellular electromagnetic fields under ultrasound, as depicted in Fig. 3(b).[194] These electrical signals boost Ca^{2+} influx in nerve cells *via* voltage-dependent L-type Ca^{2+} channels. The resultant rise in intracellular Ca^{2+} concentration leads to phosphorylation of tyrosine hydroxylase and heightened hydroxylase activity.[195] This piezoelectric effect modulates neural plasticity, aiding in the recovery of degenerative dopaminergic neurons in the midbrain.

5 Piezoelectric 2D nanosheets for future drug delivery applications

Piezoelectric 2D nanomaterials are emerging as effective agents in targeted regenerative drug delivery systems. They release drugs at specific sites in response to mechanical stimuli like ultrasound,[106] friction,[196] and vibration.[197] These nanomaterials, with their adaptable surface properties, are increasingly used in intelligent drug delivery for biomedical applications.[41,198] They offer more active sites and unique action mechanisms compared to other materials. These nanomaterials interact with protons,[199,200] substrates,[201] enzymes,[202] and cell surface proteins and lipids, facilitating piezoelectric responsiveness and microcurrent stimulation. They can anchor nanodrugs to cellular membranes using antibodies and aptamers.[203–206]

Furthermore, piezoelectric nanomaterials play a significant role in controlling inflammation and maintaining immune microenvironment homeostasis at nano-bio interfaces.[34] Piezoelectric 2D nanosheet drug release systems are being combined with polymers,[207] biomolecules,[208,209] and nanodots[210] to create multifunctional materials. Various 2D materials exhibiting piezoelectricity show promise in drug delivery nanoplatforms and as therapeutic agents, including metal–organic frameworks,[211] graphene,[212] black phosphorus,[209] BN,[213] transition metal oxides,[214] MXenes,[198] TMDCs,[215] and layered double hydroxides (LDH).[216]

5.1 Wearable and implantable devices

Electroactive materials can control drug release by electrically activating the release of adsorbed molecules. This method allows fine-tuning of release kinetics through the applied potential's magnitude, ensuring the drug delivery systems respond to physiologically safe mechanical forces without interference from daily human activities. Recently, Su *et al.* introduced a stretchable electronic facial mask (SEFM) to enhance the delivery of large-sized hyaluronic acid molecules for facial healthcare (Fig. 4(a)).[55] Utilizing sonophoresis, which increases skin permeability for a wide range of molecular sizes without harming living cells, the SEFM has proven effective in animal/human experiments. It notably increased human facial skin moisture by 20%. These developments affirm the potential of piezoelectric-stimuli materials in localized controlled drug release.

Piezoelectricity-based controlled release systems can import not only large molecules but also small molecules. A self-sufficient, subcutaneous implant, controlled by the push-button and powered by finger pressure, has been developed, enabling the release of biopharmaceuticals without the need for complex electronics and external energy (Fig. 4(b)).[217] This implant, featuring a piezoelectric membrane, facilitates the rapid and adjustable release of drugs from engineered cells, effectively normalizing blood sugar levels in a diabetic mouse model.

Furthermore, a wearable drug delivery device has been designed to achieve delicate contact on the nanoscale interfaces between materials and cells (Fig. 4(c)).[218] With a sufficiently high local electric field in the limited area of the nanoneedle–cell interface, the device shows elevated delivery efficiency and minimal damage caused to cells. The integrated system achieves efficient delivery (up to 90%) of exogenous materials into different types of cells, with cell viability over 94%. These results demonstrate that the 'nano-bio' interaction enables precise and safe drug release.
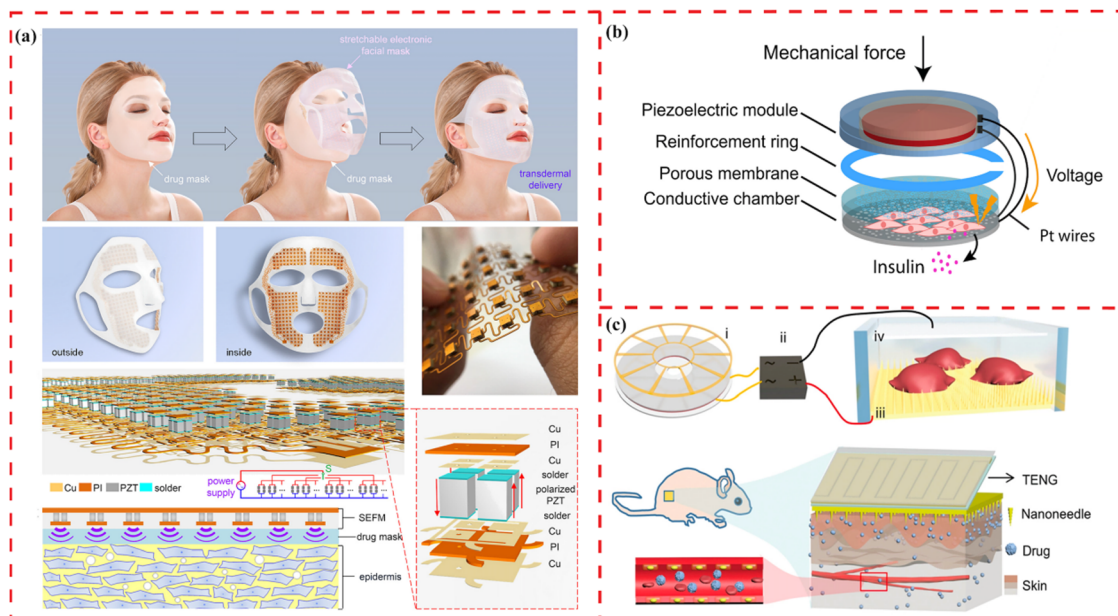
Fig. 4 Illustrations of wearable and implantable devices for drug delivery using piezoelectric materials. (a) Schematic illustration of a stretchable electronic facial mask as a platform for facial healthcare enabling the promotion of the delivery effect. Reprinted with permission from ref. 55. Copyright 2022, American Chemical Society. (b) Schematic illustration of a push button–controlled rapid drug delivery system from a piezoelectrically activated subcutaneous cell implant. Reprinted with permission from ref. 217. Copyright 2022, American Association for the Advancement of Science. (c) Schematic illustration of the *in vitro* electroporation and the *in vivo* electroporation system of a TENG-driven electroporation system to enhance delivery efficiency with minimized impairment to cell viability. Reprinted with permission from ref. 218. Copyright 2019, Wiley-VCH Verlag GmbH & Co. KGaA, Weinheim.

5.2 Targeted drug delivery systems

The rapid development of nanodrug delivery systems has initiated a revolution in tissue engineering.[219,220] They can effectively stimulate cellular responses at the nanoscale with improved drug loading efficiency, targeted capability and uptake rate.[35,221] Owing to both direct and indirect piezoelectric effects, mechanical and electrical energy can be effectively harnessed in the design of drug-release media.

Mechanical energy-mediated drug delivery and release. A smart nanoeel has been designed according to the coupled concept of the piezoelectric effect and electromagnetism (Fig. 5(a)).[32] Once alternating magnetic fields are applied, the magnetic Ni head module oscillates, subsequently causing the ferroelectric tail to flex and generating electric polarization changes *via* the piezoelectric effect. It is possible to precisely steer the nanoeels to the targeted location and trigger drug release by switching the magnetic field. Under magnetic fields of 15 mT and 11 Hz, the carriers remained in swimming mode, whereas doxorubicin release could not be observed. In contrast, in the drug release mode of 10 mT and 7 Hz, doxorubicin delivered into the cancer cells can be observed. Similarly, magneto-piezoelectric Janus particle-based micromachines have been fabricated to precisely control nanorobot motions under magnetic fields.[31]

Electrical energy-mediated drug release. Unlike devices releasing drugs based on the indirect piezoelectric effect, the electrical signals generated *via* the direct piezoelectric effect can trigger drug release by charge repulsion. A targeted nanoscale platform has been fabricated to treat glioblastoma

multiforme according to the responsive release of molecules under the piezoelectric effect.[222] Functionalized P(VDF-TrFE) nanoparticles loaded with the small-molecule inhibitor nutlin-3a were designed for antitumour treatment *in vivo*. The nanoparticles can be remotely activated by ultrasound-based mechanical stimuli to induce drug release and deliver anticancer electric signals.

Flexible FeGa@P(VDF-TrFE) core–shell magnetoelectric nanowires have demonstrated that they can be actuated by different magnetic fields for targeted drug delivery.[16] Upon magnetic stimulation, the magnetostrictive FeGa core deforms. The strain transferred onto the piezoelectric P(VDF-TrFE) shell induces surface polarization and releases the loaded paclitaxel. Similarly, the piezoelectric effect can be coupled with electromagnetism to generate loco-motion and migrate to the targeted cells,[30] as shown in Fig. 5(b). Subject to the appropriate magnetic stimulation, magnetoelectric materials change their electric polarization, induce surface charge redistribution and trigger chemical processes.

5.3 Controlled molecule release

Growth factors, key elements in tissue engineering, stimulate cell differentiation, migration and proliferation.[223,224] Bioactive ions, such as Zn^{2+},[225] Mg^{2+}[226] and Sr^{2+},[227] have been identified to regulate cell metabolism and tissue regeneration either alone or in combination with growth factors. Due to the short half-life, growth factors and bioactive ions require targeted delivery and a precise release pattern.[228]

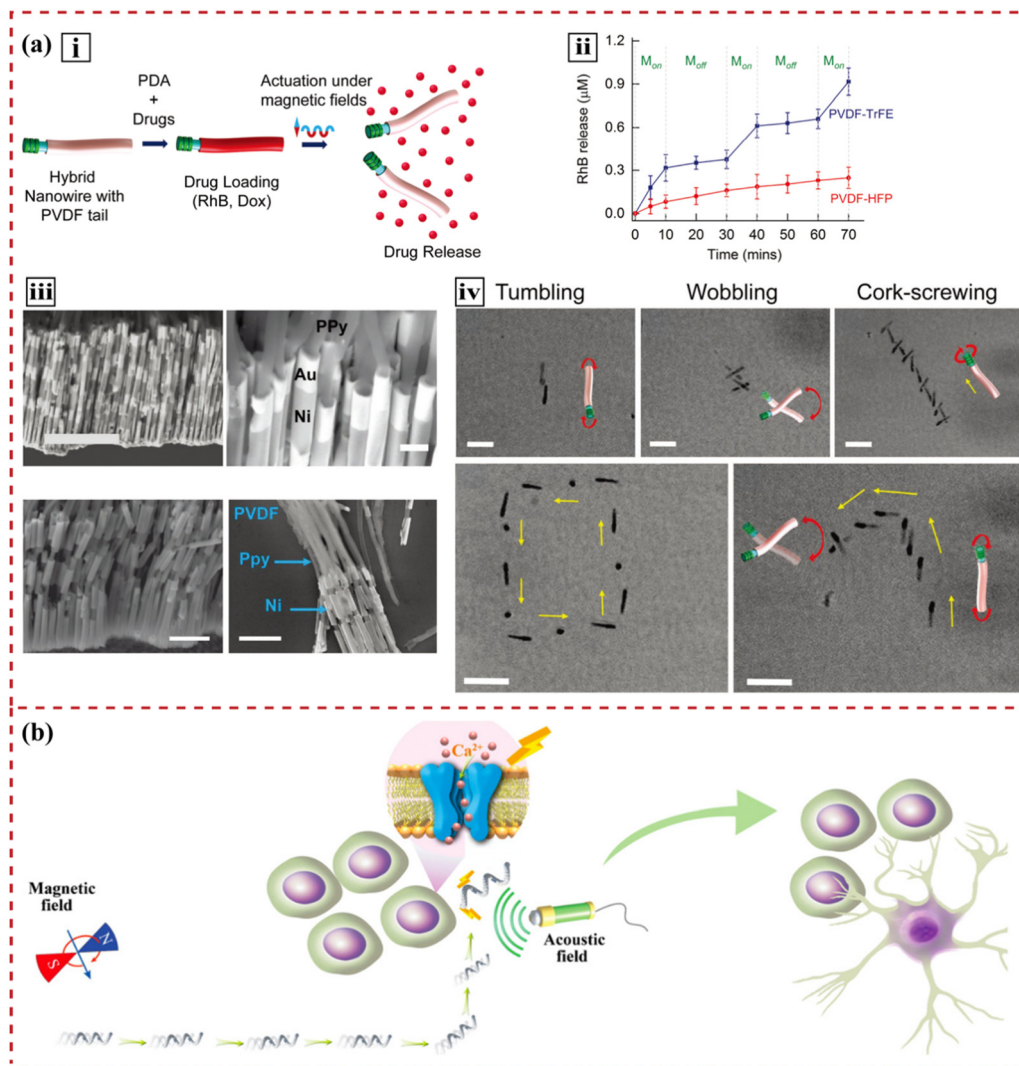2D materials are attractive substrates for protein immobilization.[41] The high protein adsorption capacity is

Fig. 5   Illustration of targeted drug delivery systems using piezoelectric materials. (a) Images of a soft hybrid nanowire that mimics an electric eel to deliver drugs in a controlled manner. (i) Scheme depicting functionalization of hybrid nanoeels with polydopamine and drugs, followed by magnetically triggered drug release. (ii) Continuous rhodamine-B release at 10 mT and 7 Hz shows three times higher release for the piezoelectric P(VDF-TrFE) nanowires than for the nonpiezoelectric nanowires. (iii) Steps of fabricating nanowires, characterized by SEM. (iv) Characterization of the swimming behaviors of the hybrid nanowires. Reprinted with permission from ref. 32. Copyright 2019, Wiley-VCH Verlag GmbH & Co. KGaA, Weinheim. (b) Schematic illustration of a highly controllable micromotor to induce targeted neural stem-like cell differentiation. Reprinted with permission from ref. 30. Copyright 2020, Wiley-VCH Verlag GmbH & Co. KGaA, Weinheim.

supported by the large area-to-volume ratio of 2D materials.[229] The atomic thickness provided mechanical flexibility for interactions between the material surface and adsorbed protein. Other surface characteristics, including functionality, crystallinity and curvature, can be altered to regulate protein adsorption and profoundly influence material–protein interactions.[41,229]

A piezoelectric polymer (poly(3-hydroxybutyrate)) loaded with silica microcapsules is investigated, demonstrating its capability to anchor bioactive molecules (such as bovine serum albumin) onto the scaffold surface.[230] The change in surface charges, brought about by the matrix's piezoelectric properties, favors the adherence of more bioactive compounds. An investigation into the impact of ultrasound, enzymes, and laser radiation on initiating reactions reveals that ultrasound

(20 kHz, 50 W for 120 s) rapidly alters the kinetic profile of the drug. According to piezoelectric $Pb[Zr_{(x)}Ti_{(1-x)}]O_3$ and biocompatible polydimethylsiloxane (PDMS), Tseng $et\ al.$ fabricated a flexible and stretchable electronic device for drug delivery.[231] The advantages of piezoelectric 2D nanosheet flexibility and stretchability in drug release applications have been proven.

Piezoelectricity has been proven to boost interfacial cation transport in a controlled way. Zhang $et\ al.$ have designed an integrative material built using a piezoelectric–dielectric flexible PVDF film that involves reduced graphene oxide 2D nanosheet fillers.[232] The enhanced release may be attributed to the release of charged small molecules, which are produced by random and alternating positive/negative piezoelectric potentials under mechanical disturbances. They have also

developed a similar enzyme release system that preserves enzyme activities.[233] All the devices can be utilized in active drug release by responding to extensive mechanical disturbances of human movement.

Furthermore, piezocatalysis offers a viable approach for prodrug activation. The employment of piezoelectric 2D nanocarriers for prodrug loading enables not only efficient delivery to targeted sites but also increased concentration of prodrugs at these specific locations.[234] Under the influence of ultrasound, the catalytic action facilitated by piezoelectric 2D nanomaterials converts inactive prodrugs into highly active pharmaceutical compounds, thus enabling targeted and precise drug therapy.[235]

6 Conclusions and perspectives

Since the demonstration of the piezoelectric properties of MoS_2 2D nanosheets, 2D-structural piezoelectric nanomaterials have become popular in sensing, catalysis, energy and biomedicine areas. The strong targeting ability and minimized side effects are major advantages of these nanoscale drug delivery systems. In this review, the potential suitability of piezoelectric 2D nanosheets for drug delivery systems is discussed. When seeking solutions for more structurally demanding targets, such as bone defects and nerve injuries, the remote fields, for example, the acoustic fields, can provide biomedical modes in driving directional or local cell responses within *in vivo* tissue culture. On the one hand, the piezoelectric 2D nanosheet inside the human body can act as an energy converter to generate electrical signals without an open wound when applying an acoustic field. These essential electrical cues can trigger osteogenic-/neurogenic-related cell pathways or alter the local microenvironment to switch on the regenerative mode. Conversely, in the absence of remote fields, 2D nanosheets are capable of harvesting energy from cellular activity and modulating cell behaviors. This process inherently represents a method of inverse entropy increase in energy dissipation.

Moreover, piezoelectric 2D nanosheets can interact with the fundamental components of tissue regeneration: cells, materials, and biochemical factors. For cells, ultrathin electrical 2D nanosheets can build a unique nano-bio interface for cell activation. Regarding materials, 2D nanosheets can either be considered as standalone entities or employed as enhancements for scaffold materials. By connecting the scaffold material with the seed cells, the scaffolds can be functionalized for precise regulation. For biochemical factors (*i.e.*, ions and proteins), 2D nanosheets can be transformed into drug delivery systems. The vast canvas – the large surface of the 2D structure – provides active sites for molecular binding and is beneficial for drug loading, tissue targeting and stimulus response. The controllable surface polarization brings programmable electrical signals, guaranteeing a release pattern of bioactive molecules.

For tumor treatment, piezocatalysis of 2D nanosheets can provide a synergistic effect with therapeutic drugs. Piezocatalysis causes ROS generation and glutathione depletion in tumor cells, leading to a sharp decrease in the activities of tumor cells.

Stimuli-responsive released chemotherapeutic or immunotherapeutic drugs can obtain excellent antitumour effects. In addition, piezoelectric-related water splitting can remodel the tumor microenvironment by reducing tumor interstitial pressure, thereby achieving deep penetration of drugs. The treatment of degenerative diseases can be conducted in the same way. Given that piezoelectric 2D nanosheets can harvest energy from the surrounding subtle mechanical cues, drug delivery systems with high piezoelectric coefficients can even have a sustainable treatment effect after removing the external stimulus, realizing energy recycling.

Therefore, considering the increasing mechanisms and applications of piezoelectric 2D nanosheets being revealed, this review aims to build bridges between diverse academic disciplines. Looking towards the future of drug delivery, the design of drug delivery systems should ideally adopt a top-down approach, emphasizing energy-efficient fabrication and the attainment of effective functionalities. Using piezoelectric 2D nanosheets as an example, it is possible to discover multiple functions of a single material from various perspectives across different fields. This may simplify the complicated design and fabrication of drug delivery systems and optimize the applications of nanoscale drug delivery systems.

Conflicts of interest

There are no conflicts to declare.

Acknowledgements

References

1 M. S. Alqahtani, M. Kazi, M. A. Alsenaidy and M. Z. Ahmad, *Front. Pharmacol.*, 2021, **12**, 618411.

2 H. Marwah, T. Garg, A. K. Goyal and G. Rath, *Drug Delivery*, 2016, **23**, 564–578.

3 M. Ying-Yan, L. Meng, W. Jin-Da, W. Kai-Jie, Z. Jing-Shang, C. Shu-Ying, L. Xu, L. Qing-Feng, G. Fei and W. Xiu-Hua, *J. Controlled Release*, 2021, **339**, 391–402.

4 K. Albinali, M. Zagho, Y. Deng and A. Elzatahry, *Int. J. Nanomed.*, 2019, **14**, 1707–1723.

5 R. Avila, C. Li, Y. Xue, J. A. Rogers and Y. Huang, *Proc. Natl. Acad. Sci. U. S. A.*, 2021, **118**, e2026405118.

6 K. Kapat, Q. T. H. Shubhra, M. Zhou and S. Leeuwenburgh, *Adv. Funct. Mater.*, 2020, **30**, 1909045.

7 L. Edgar, T. Pu, B. Porter, J. M. Aziz, C. La Pointe, A. Asthana and G. Orlando, *Br. J. Surg.*, 2020, **107**, 793–800.

8 F. Berthiaume, T. J. Maguire and M. L. Yarmush, *Annu. Rev. Chem. Biomol. Eng.*, 2011, **2**, 403–430.

9 S. Yao, M. Zheng, Z. Wang, Y. Zhao, S. Wang, Z. Liu, Z. Li, Y. Guan, Z. L. Wang and L. Li, *Adv. Mater.*, 2022, 2205881.

10 P. Li, Y. Bräuniger, J. Kunigkeit, M. R. O. Vega, E. Zhang, J. Grothe and S. Kaskel, *Angew. Chem., Int. Ed.*, 2022, **61**, 10.

11 M. Hasan, A. Khatun, T. Fukuta and K. Kogure, *Adv. Drug Delivery Rev.*, 2020, **154–155**, 227–235.

12 M. Toyoda, S. Hama, Y. Ikeda, Y. Nagasaki and K. Kogure, *Int. J. Pharm.*, 2015, **483**, 110–114.

13 W.-C. Huang, C.-C. Lin, T.-W. Chiu and S.-Y. Chen, *ACS Appl. Mater. Interfaces*, 2022, **14**, 46188–46200.

14 M. Mishra, G. Sen Gupta and X. Gui, *Sensors*, 2022, **22**, 7685.

15 J. M. Marmolejo-Tejada, J. De La Roche-Yepes, C. A. Pérez-López, J. A. P. Taborda, A. Ávila and A. Jaramillo-Botero, *J. Chem. Inf. Model.*, 2021, **61**, 4537–4543.

16 P. Lin, C. Pan and Z. L. Wang, *Mater. Today Nano*, 2018, **4**, 17–31.

17 J. Tao, Y. Chen, A. Bhardwaj, L. Wen, J. Li, O. V. Kolosov, Y. Lin, Z. Hong, Z. Huang and S. Mathur, *Proc. Natl. Acad. Sci. U. S. A.*, 2022, **119**, e2211059119.

18 M. T. Chorsi, E. J. Curry, H. T. Chorsi, R. Das, J. Baroody, P. K. Purohit, H. Ilies and T. D. Nguyen, *Adv. Mater.*, 2019, **31**, 1802084.

19 M. Lee, J. R. Renshof, K. J. van Zeggeren, M. J. A. Houmes, E. Lesne, M. Šiškins, T. C. van Thiel, R. H. Guis, M. R. van Blankenstein, G. J. Verbiest, A. D. Caviglia, H. S. J. van der Zant and P. G. Steeneken, *Adv. Mater.*, 2022, 2204630.

20 X. Li, Y. Li, Y. Li, J. Tan, J. Zhang, H. Zhang, J. Liang, T. Li, Y. Liu, H. Jiang and P. Li, *ACS Appl. Mater. Interfaces*, 2022, **14**, 46789–46800.

21 Y. Dobashi, D. Yao, Y. Petel, T. N. Nguyen, M. S. Sarwar, Y. Thabet, C. L. W. Ng, E. Scabeni Glitz, G. T. M. Nguyen, C. Plesse, F. Vidal, C. A. Michal and J. D. W. Madden, *Science*, 2022, **376**, 502–507.

22 Y. Zhang, H. Zhang, L. Chen, J. Wang, J. Wang, J. Li, Y. Zhao, M. Zhang and H. Zhang, *Environ. Sci. Technol.*, 2022, **56**, 16271–16280.

23 K. Wang, C. Han, J. Li, J. Qiu, J. Sunarso and S. Liu, *Angew. Chem., Int. Ed.*, 2022, **61**, e202110429.

24 J. M. Wu, W. E. Chang, Y. T. Chang and C. Chang, *Adv. Mater.*, 2016, **28**, 3718–3725.

25 A. Cafarelli, A. Marino, L. Vannozzi, J. Puigmartí-Luis, S. Pané, G. Ciofani and L. Ricotti, *ACS Nano*, 2021, **15**, 11066–11086.

26 R. Sun, M. Liu, J. Lu, B. Chu, Y. Yang, B. Song, H. Wang and Y. He, *Nat. Commun.*, 2022, **13**, 5127.

27 L. Wang, Y. Shi, J. Jiang, C. Li, H. Zhang, X. Zhang, T. Jiang, L. Wang, Y. Wang and L. Feng, *Small*, 2022, 2203678.

28 M. Yu, W. Yang, W. Yue and Y. Chen, *Adv. Sci.*, 2022, 2204335.

29 A. Li, W. Gao, X. Zhang, Y. Deng, Y. Zhu, H. Gu, J. Wen and X. Jiang, *Biomater. Adv.*, 2022, **138**, 212935.

30 L. Liu, B. Chen, K. Liu, J. Gao, Y. Ye, Z. Wang, N. Qin, D. A. Wilson, Y. Tu and F. Peng, *Adv. Funct. Mater.*, 2020, **30**, 1910108.

31 X.-Z. Chen, N. Shamsudhin, M. Hoop, R. Pieters, E. Siringil, M. S. Sakar, B. J. Nelson and S. Pané, *Mater. Horiz.*, 2016, **3**, 113–118.

32 F. Mushtaq, H. Torlakcik, M. Hoop, B. Jang, F. Carlson, T. Grunow, N. Läubli, A. Ferreira, X. Chen, B. J. Nelson and S. Pané, *Adv. Funct. Mater.*, 2019, **29**, 1808135.

33 C. Li, Z. Xiong, L. Zhou, W. Huang, Y. He, L. Li, H. Shi, J. Lu, J. Wang, D. Li and S. Yin, *Adv. Healthcare Mater.*, 2022, **11**, 2201471.

34 G. Peng and B. Fadeel, *Adv. Drug Delivery Rev.*, 2022, **188**, 114422.

35 Z. Li, X. Zhu, J. Li, J. Zhong, J. Zhang and J. Fan, *Nanoscale*, 2022, **14**, 5384–5391.

36 Y. Meng, H. Zhong, Z. Xu, T. He, J. S. Kim, S. Han, S. Kim, S. Park, Y. Shen, M. Gong, Q. Xiao and S.-H. Bae, *Nanoscale Horiz.*, 2023, **8**, 1345–1365.

37 X. Yang, C. Shang, S. Zhou and J. Zhao, *Nanoscale Horiz.*, 2020, **5**, 1106–1115.

38 L. Qi, S. Ruan and Y. Zeng, *Adv. Mater.*, 2021, **33**, 2005098.

39 A. Corletto, A. V. Ellis, N. A. Shepelin, M. Fronzi, D. A. Winkler, J. G. Shapter and P. C. Sherrell, *Adv. Mater.*, 2022, **34**, 2203849.

40 A. B. Puthirath, X. Zhang, A. Krishnamoorthy, R. Xu, F. S. Samghabadi, D. C. Moore, J. Lai, T. Zhang, D. E. Sanchez, F. Zhang, N. R. Glavin, D. Litvinov, R. Vajtai, V. Swaminathan, M. Terrones, H. Zhu, P. Vashishta and P. M. Ajayan, *Adv. Mater.*, 2022, **34**, 2206425.

41 S. H. Chen, D. R. Bell and B. Luan, *Adv. Drug Delivery Rev.*, 2022, **186**, 114336.

42 X. He, Y. Zhu, B. Ma, X. Xu, R. Huang, L. Cheng and R. Zhu, *Adv. Drug Delivery Rev.*, 2022, **187**, 114379.

43 M. Zhao, X. Gao, J. Wei, C. Tu, H. Zheng, K. Jing, J. Chu, W. Ye and T. Groth, *Front. Bioeng. Biotechnol.*, 2022, **10**, 991855.

44 B. Das, S. Maity, S. Paul, K. Dolui, S. Paramanik, S. Naskar, S. R. Mohanty, S. Chakraborty, A. Ghosh, M. Palit, K. Watanabe, T. Taniguchi, K. S. R. Menon and S. Datta, *ACS Nano*, 2021, **15**, 20203–20213.

45 Y. Wu, S. Dong, N. Lv, Z. Xu, R. Ren, G. Zhu, B. Huang, Y. Zhang and X. Dong, *Small*, 2022, 2204888.

46 S. Xiao, Y. Zheng, X. Wu, M. Zhou, X. Rong, L. Wang, Y. Tang, X. Liu, L. Qiu and C. Cheng, *Small*, 2022, **18**, 2203281.

47 M. Li, Y. Gao, X. Fan, Y. Wei, Q. Hao and T. Qiu, *Nanoscale Horiz.*, 2021, **6**, 186–191.

48 C. Dai, R. Hu, C. Wang, Z. Liu, S. Zhang, L. Yu, Y. Chen and B. Zhang, *Nanoscale Horiz.*, 2020, **5**, 857–868.

49 S. Li, Z. Zhao, J. Li, H. Liu, M. Liu, Y. Zhang, L. Su, A. I. Pérez-Jiménez, Y. Guo, F. Yang, Y. Liu, J. Zhao, J. Zhang, L. Zhao and Y. Lin, *Small*, 2022, **18**, 2202507.

50 Z. Ye, Y. Fan, T. Zhu, D. Cao, X. Hu, S. Xiang, J. Li, Z. Guo, X. Chen, K. Tan and N. Zheng, *ACS Appl. Mater. Interfaces*, 2022, **14**, 23194–23205.

51 Y. Kang, Z. Mao, Y. Wang, C. Pan, M. Ou, H. Zhang, W. Zeng and X. Ji, *Nat. Commun.*, 2022, **13**, 2425.

52 P. Ma, X. Lai, Z. Luo, Y. Chen, X. J. Loh, E. Ye, Z. Li, C. Wu and Y.-L. Wu, *Nanoscale Adv.*, 2022, **4**, 3462–3478.

53 B. T. Mai, J. S. Conteh, H. Gavilán, A. Di Girolamo and T. Pellegrino, *ACS Appl. Mater. Interfaces*, 2022, **14**, 48476–48488.

54 J. P. K. Armstrong and M. M. Stevens, *Trends Biotechnol.*, 2020, **38**, 254–263.

55 S. Li, J. Xu, R. Li, Y. Wang, M. Zhang, J. Li, S. Yin, G. Liu, L. Zhang, B. Li, Q. Gu and Y. Su, *ACS Nano*, 2022, **16**, 5961–5974.

56 X. Li, B. C. Heng, Y. Bai, Q. Wang, M. Gao, Y. He, X. Zhang, X. Deng and X. Zhang, *Bioact. Mater.*, 2023, **20**, 81–92.

57 X. Dai, B. C. Heng, Y. Bai, F. You, X. Sun, Y. Li, Z. Tang, M. Xu, X. Zhang and X. Deng, *Bioact. Mater.*, 2021, **6**, 2029–2038.

58 M. B. Ghasemian, T. Daeneke, Z. Shahrbabaki, J. Yang and K. Kalantar-Zadeh, *Nanoscale*, 2020, **12**, 2875–2901.

59 M.-M. Yang, Z.-D. Luo, Z. Mi, J. Zhao, S. P. E and M. Alexe, *Nature*, 2020, **584**, 377–381.

60 S. Bairagi and S. W. Ali, *Energy*, 2020, **198**, 117385.

61 X. Zuo, K. Chang, J. Zhao, Z. Xie, H. Tang, B. Li and Z. Chang, *J. Mater. Chem. A*, 2016, **4**, 51–58.

62 L. Liang, C. Sun, R. Zhang, S. Han, J. Wang, N. Ren and H. Liu, *Nano Energy*, 2021, **90**, 106634.

63 J. Wang, D. Adami, B. Lu, C. Liu, A. Maazouz and K. Lamnawar, *Polymers*, 2020, **12**, 2596.

64 Y. Liu, W.-G. Liu, D.-B. Lin, X.-L. Niu, S. Zhou, J. Zhang, S.-B. Ge, Y.-C. Zhu, X. Meng and Z.-L. Chen, *Nanomaterials*, 2022, **12**, 588.

65 Z.-X. Wang and W.-Q. Liao, *Science*, 2022, **375**, 1353–1354.

66 Y. Su, W. Li, X. Cheng, Y. Zhou, S. Yang, X. Zhang, C. Chen, T. Yang, H. Pan, G. Xie, G. Chen, X. Zhao, X. Xiao, B. Li, H. Tai, Y. Jiang, L.-Q. Chen, F. Li and J. Chen, *Nat. Commun.*, 2022, **13**, 4867.

67 W. Wu, L. Wang, Y. Li, F. Zhang, L. Lin, S. Niu, D. Chenet, X. Zhang, Y. Hao, T. F. Heinz, J. Hone and Z. L. Wang, *Nature*, 2014, **514**, 470–474.

68 L. Rogée, L. Wang, Y. Zhang, S. Cai, P. Wang, M. Chhowalla, W. Ji and S. P. Lau, *Science*, 2022, **376**, 973–978.

69 V. J. González, A. M. Rodríguez, I. Payo and E. Vázquez, *Nanoscale Horiz.*, 2020, **5**, 331–335.

70 S. Rahman and Y. Lu, *Nanoscale Horiz.*, 2022, **7**, 849–872.

71 G. Cheon, K.-A. N. Duerloo, A. D. Sendek, C. Porter, Y. Chen and E. J. Reed, *Nano Lett.*, 2017, **17**, 1915–1923.

72 M. Zelisko, Y. Hanlumyuang, S. Yang, Y. Liu, C. Lei, J. Li, P. M. Ajayan and P. Sharma, *Nat. Commun.*, 2014, **5**, 4284.

73 D. Kim, S. A. Han, J. H. Kim, J. Lee, S. Kim and S. Lee, *Adv. Mater.*, 2020, **32**, 1906989.

74 S. Guerin, A. Stapleton, D. Chovan, R. Mouras, M. Gleeson, C. McKeown, M. R. Noor, C. Silien, F. M. F. Rhen, A. L. Kholkin, N. Liu, T. Soulimane, S. A. M. Tofail and D. Thompson, *Nat. Mater.*, 2018, **17**, 180–186.

75 P. Zelenovskiy, D. Vasileva, A. Nuraeva, S. Vasilev, T. Khazamov, E. Dikushina, V. Ya Shur and A. L. Kholkin, *Ferroelectrics*, 2016, **496**, 10–19.

76 R. M. F. Baptista, E. de Matos Gomes, M. M. M. Raposo, S. P. G. Costa, P. E. Lopes, B. Almeida and M. S. Belsley, *Nanoscale Adv.*, 2019, **1**, 4339–4346.

77 T. Nakiri, K. Imoto, M. Ishizuka, S. Okamoto, M. Date, Y. Uematsu, E. Fukada and Y. Tajitsu, *Jpn. J. Appl. Phys.*, 2004, **43**, 6769.

78 D. Denning, M. V. Paukshto, S. Habelitz and B. J. Rodriguez, *J. Biomed. Mater. Res.*, 2014, **102**, 284–292.

79 Z. Zhang, S. Liu, Q. Pan, Y. Hong, Y. Shan, Z. Peng, X. Xu, B. Liu, Y. Chai and Z. Yang, *Adv. Mater.*, 2022, **34**, 2200864.

80 V. Vivekananthan, N. R. Alluri, Y. Purusothaman, A. Chandrasekhar, S. Selvarajan and S.-J. Kim, *ACS Appl. Mater. Interfaces*, 2018, **10**, 18650–18656.

81 J. Ohnuki, T. Sato and M. Takano, *Phys. Rev. E*, 2016, **94**, 012406.

82 B. D. Ratner and F. J. Schoen, *Biomaterials Science*, Elsevier, 2020, pp. 843–849.

83 N. Wiesmann, W. Tremel and J. Brieger, *J. Mater. Chem. B*, 2020, **8**, 4973–4989.

84 J. Sun, H. Guo, J. Ribera, C. Wu, K. Tu, M. Binelli, G. Panzarasa, F. W. M. R. Schwarze, Z. L. Wang and I. Burgert, *ACS Nano*, 2020, **14**, 14665–14674.

85 A. Sood, M. Desseigne, A. Dev, L. Maurizi, A. Kumar, N. Millot and S. S. Han, *Small*, 2023, **19**, 2206401.

86 T. Webster, P. Maschhoff and B. Geilich, *Int. J. Nanomed.*, 2013, 257.

87 T. A. Hilder and N. Gaston, *ChemPhysChem*, 2016, **17**, 1573–1578.

88 S. Mateti, C. S. Wong, Z. Liu, W. Yang, Y. Li, L. H. Li and Y. Chen, *Nano Res.*, 2018, **11**, 334–342.

89 T. Liu, C. Wang, W. Cui, H. Gong, C. Liang, X. Shi, Z. Li, B. Sun and Z. Liu, *Nanoscale*, 2014, **6**, 11219–11225.

90 L. Cheng, J. Liu, X. Gu, H. Gong, X. Shi, T. Liu, C. Wang, X. Wang, G. Liu, H. Xing, W. Bu, B. Sun and Z. Liu, *Adv. Mater.*, 2014, **26**, 1886–1893.

91 X. Qian, S. Shen, T. Liu, L. Cheng and Z. Liu, *Nanoscale*, 2015, **7**, 6380–6387.

92 S. Zhu, L. Gong, J. Xie, Z. Gu and Y. Zhao, *Small Methods*, 2017, **1**, 1700220.

93 G. Liu, X. Yan, C. Li, S. Hu, J. Yan and B. Yan, *J. Hazard. Mater.*, 2023, **443**, 130303.

94 H. J. Dyson and P. E. Wright, *FASEB J.*, 1995, **9**, 37–42.

95 D. W. Kulp and W. R. Schief, *Curr. Opin. Virol.*, 2013, **3**, 322–331.

96 J. Li, Y. Long, F. Yang and X. Wang, *Curr. Opin. Solid State Mater. Sci.*, 2020, **24**, 100806.

97 W. Wang, Z. Wu, Z. Dai, Y. Yang, J. Wang and G. Wu, *Amino Acids*, 2013, **45**, 463–477.

98 K. A. Alberti and Q. Xu, *Regen Biomater.*, 2016, **3**, 1–11.

99 I. C. Amaechi, A. Hadj Youssef, A. Dörfler, Y. González, R. Katoch and A. Ruediger, *Angew. Chem., Int. Ed.*, 2022, **61**, e202207975.

100 X. Wang, J. Wu, Y. Zhang, Y. Sun, K. Ma, Y. Xie, W. Zheng, Z. Tian, Z. Kang and Y. Zhang, *Adv. Mater.*, 2022, 2206576.

101 A. Ranjan, K.-Y. Hsiao, C.-Y. Lin, Y.-H. Tseng and M.-Y. Lu, *ACS Appl. Mater. Interfaces*, 2022, **14**, 35635–35644.

102 H. Xiao, J. He, X. Lu, F. Wang and Y. Guo, *Chemosphere*, 2022, **306**, 135543.

103 P. C. Sherrell, M. Fronzi, N. A. Shepelin, A. Corletto, D. A. Winkler, M. Ford, J. G. Shapter and A. V. Ellis, *Chem. Soc. Rev.*, 2022, **51**, 650–671.

104 M. B. Ghasemian, T. Daeneke, Z. Shahrbabaki, J. Yang and K. Kalantar-Zadeh, *Nanoscale*, 2020, **12**, 2875–2901.

105 T. Zhao, S. Zhang, Y. Guo and Q. Wang, *Nanoscale*, 2016, **8**, 233–242.

106 J. Jang, K. Kim, J. Yoon and C. B. Park, *Biomaterials*, 2020, **255**, 120165.

107 Z. Li, T. Zhang, F. Fan, F. Gao, H. Ji and L. Yang, *J. Phys. Chem. Lett.*, 2020, **11**, 1228–1238.

108 K. Su, L. Tan, X. Liu, Z. Cui, Y. Zheng, B. Li, Y. Han, Z. Li, S. Zhu, Y. Liang, X. Feng, X. Wang and S. Wu, *ACS Nano*, 2020, **14**, 2077–2089.

109 X. Feng, L. Ma, J. Lei, Q. Ouyang, Y. Zeng, Y. Luo, X. Zhang, Y. Song, G. Li, L. Tan, X. Liu and C. Yang, *ACS Nano*, 2022, **16**, 2546–2557.

110 M. Xu, M. Lu, G. Qin, X. Wu, T. Yu, L. Zhang, K. Li, X. Cheng and Y. Lan, *Angew. Chem., Int. Ed.*, 2022, **61**, e202210700.

111 Y. He, Z. Xu, Y. He, G. Cao, S. Ni, Y. Tang, J. Wang, Y. Yuan, Z. Ma, D. Wang and D. Gao, *Biomaterials*, 2022, **290**, 121816.

112 M. Yoshida, *JACC*, 2022, **7**, 162–163.

113 I. Ohsawa, M. Ishikawa, K. Takahashi, M. Watanabe, K. Nishimaki, K. Yamagata, K. Katsura, Y. Katayama, S. Asoh and S. Ohta, *Nat. Med.*, 2007, **13**, 688–694.

114 S. Takeuchi, K. Nagatani, N. Otani, H. Nawashiro, T. Sugawara, K. Wada and K. Mori, *BMC Neurosci.*, 2015, **16**, 22.

115 N. Kamimura, K. Nishimaki, I. Ohsawa and S. Ohta, *Obesity*, 2011, **19**, 1396–1403.

116 W.-W. Cai, M.-H. Zhang, Y.-S. Yu and J.-H. Cai, *Mol. Cell. Biochem.*, 2013, **373**, 1–9.

117 Y. Sun, F. Shuang, D. M. Chen and R. B. Zhou, *Osteoporosis Int.*, 2013, **24**, 969–978.

118 S.-L. Huang, J. Jiao and H.-W. Yan, *Exp. Ther. Med.*, 2016, **11**, 177–182.

119 M. Iketani and I. Ohsawa, *Curr. Neuropharmacol.*, 2017, **15**, 324–331.

120 R. Pluta, S. Januszewski and S. J. Czuczwar, *Int. J. Mater. Sci.*, 2022, **23**, 6591.

121 K. Nagatani, H. Nawashiro, S. Takeuchi, S. Tomura, N. Otani, H. Osada, K. Wada, H. Katoh, N. Tsuzuki and K. Mori, *Med. Gas Res.*, 2013, **3**, 13.

122 L. Zhang, P. Zhao, C. Yue, Z. Jin, Q. Liu, X. Du and Q. He, *Biomaterials*, 2019, **197**, 393–404.

123 Z. Jin, Y. Sun, T. Yang, L. Tan, P. Lv, Q. Xu, G. Tao, S. Qin, X. Lu and Q. He, *Biomaterials*, 2021, **276**, 121030.

124 S. Chen, Y. Zhu, Q. Xu, Q. Jiang, D. Chen, T. Chen, X. Xu, Z. Jin and Q. He, *Nat. Commun.*, 2022, **13**, 5684.

125 T. W. LeBaron, I. Laher, B. Kura and J. Slezak, *Can. J. Physiol. Pharmacol.*, 2019, **97**, 797–807.

126 P. Agostinis, K. Berg, K. A. Cengel, T. H. Foster, A. W. Girotti, S. O. Gollnick, S. M. Hahn, M. R. Hamblin, A. Juzeniene, D. Kessel, M. Korbelik, J. Moan, P. Mroz, D. Nowis, J. Piette, B. C. Wilson and J. Golab, *Ca-Cancer J. Clin.*, 2011, **61**, 250–281.

127 H.-H. Kim and S. Choi, *Int. J. Mater. Sci.*, 2018, **19**, 2381.

128 L. Wu and R. Wang, *Pharmacol. Rev.*, 2005, **57**, 585–630.

129 Y. You, Y.-X. Zhu, J. Jiang, M. Wang, Z. Chen, C. Wu, J. Wang, W. Qiu, D. Xu, H. Lin and J. Shi, *J. Am. Chem. Soc.*, 2022, **144**, 14195–14206.

130 D. J. Selkoe and J. Hardy, *EMBO Mol. Med.*, 2016, **8**, 595–608.

131 D. Brambilla, R. Verpillot, B. Le Droumaguet, J. Nicolas, M. Taverna, J. Kóňa, B. Lettiero, S. H. Hashemi, L. De Kimpe, M. Canovi, M. Gobbi, V. Nicolas, W. Scheper, S. M. Moghimi, I. Tvaroška, P. Couvreur and K. Andrieux, *ACS Nano*, 2012, **6**, 5897–5908.

132 J. Lei, C. Wang, X. Feng, L. Ma, X. Liu, Y. Luo, L. Tan, S. Wu and C. Yang, *Chem. Eng. J.*, 2022, **435**, 134624.

133 Z. Yuan, B. Tao, Y. He, J. Liu, C. Lin, X. Shen, Y. Ding, Y. Yu, C. Mu, P. Liu and K. Cai, *Biomaterials*, 2019, **217**, 119290.

134 X. Feng, J. Lei, L. Ma, Q. Ouyang, Y. Zeng, H. Liang, C. Lei, G. Li, L. Tan, X. Liu and C. Yang, *Small*, 2022, **18**, 2105775.

135 Y. He, Z. Xu, Y. He, G. Cao, S. Ni, Y. Tang, J. Wang, Y. Yuan, Z. Ma, D. Wang and D. Gao, *Biomaterials*, 2022, **290**, 121816.

136 A. Wu, L. Jiang, C. Xia, Q. Xu, B. Zhou, Z. Jin, Q. He and J. Guo, *Adv. Sci.*, 2023, **10**, 2303016.

137 P. Lheritier, A. Torelló, T. Usui, Y. Nouchokgwe, A. Aravindhan, J. Li, U. Prah, V. Kovacova, O. Bouton, S. Hirose and E. Defay, *Nature*, 2022, **609**, 718–721.

138 D. Tan, X. Cao, J. Huang, Y. Peng, L. Zeng, Q. Guo, N. Sun, S. Bi, R. Ji and C. Jiang, *Adv. Sci.*, 2022, **9**, 2201443.

139 N. A. Kamel, *Biophys. Rev.*, 2022, **14**, 717–733.

140 S. Roy, K. A. Deo, K. A. Singh, H. P. Lee, A. Jaiswal and A. K. Gaharwar, *Adv. Drug Delivery Rev.*, 2022, **187**, 114361.

141 G. Murillo, A. Blanquer, C. Vargas-Estevez, L. Barrios, E. Ibáñez, C. Nogués and J. Esteve, *Adv. Mater.*, 2017, **29**, 1605048.

142 C. Zhang, W. Wang, X. Hao, Y. Peng, Y. Zheng, J. Liu, Y. Kang, F. Zhao, Z. Luo, J. Guo, B. Xu, L. Shao and G. Li, *Adv. Funct. Mater.*, 2021, **31**, 2007487.

143 J. Chen, L. Song, F. Qi, S. Qin, X. Yang, W. Xie, K. Gai, Y. Han, X. Zhang, Z. Zhu, H. Cai, X. Pei, Q. Wan, N. Chen, J. Wang, Q. Wang and Y. Li, *Nano Energy*, 2023, **106**, 108076.

144 M. Sekkarapatti Ramasamy, V. Krishnamoorthi Kaliannagounder, A. Rahaman, C. H. Park, C. S. Kim and B. Kim, *ACS Biomater. Sci. Eng.*, 2022, **8**, 3542–3556.

145 J. Zeng, C. Gu, X. Geng, K. Lin, Y. Xie and X. Chen, *Biomaterials*, 2023, **297**, 122122.

146 Y. Yu, H. Sun, Q. Lu, J. Sun, P. Zhang, L. Zeng, K. Vasilev, Y. Zhao, Y. Chen and P. Liu, *J. Nanobiotechnol.*, 2023, **21**, 193.

147 L. Ma, X. Zhang, H. Wang, X. Feng, J. Lei, Y. He, J. Wei, Y. Zhang, L. Tan and C. Yang, *Sci. China Mater.*, 2023, **66**, 2913–2924.

148 C. Mao, W. Jin, Y. Xiang, Y. Zhu, J. Wu, X. Liu, S. Wu, Y. Zheng, K. M. C. Cheung and K. W. K. Yeung, *Adv. Mater.*, 2023, **35**, 2208681.

149 Q. Truong Hoang, K. A. Huynh, T. G. Nguyen Cao, J. H. Kang, X. N. Dang, V. Ravichandran, H. C. Kang, M. Lee, J. Kim, Y. T. Ko, T. I. Lee and M. S. Shim, *Adv. Mater.*, 2023, **35**, 2300437.

150 L. Xia, J. Chen, Y. Xie, S. Zhang, W. Xia, W. Feng and Y. Chen, *J. Mater. Chem. B*, 2023, **11**, 2895–2903.

151 C. Dai, S. Zhang, Z. Liu, R. Wu and Y. Chen, *ACS Nano*, 2017, **11**, 9467–9480.

152 S. Lin, M. Yang, J. Chen, W. Feng, Y. Chen and Y. Zhu, *Small*, 2023, **19**, 2204992.

153 L. Jiang, G. Lu, Y. Zeng, Y. Sun, H. Kang, J. Burford, C. Gong, M. S. Humayun, Y. Chen and Q. Zhou, *Nat. Commun.*, 2022, **13**, 3853.

154 D. I. Kim, R. H. Jeong, J. W. Lee, S. Park and J.-H. Boo, *Funct. Mater. Lett.*, 2021, **14**, 2151020.

155 A. Rubinacci, M. Covini, C. Bisogni, I. Villa, M. Galli, C. Palumbo, M. Ferretti, M. A. Muglia and G. Marotti, *Am. J. Physiol.: Endocrinol. Metab.*, 2002, **282**, E851–E864.

156 W. R. Walsh and N. Guzelsu, *Biomaterials*, 1993, **14**, 331–336.

157 D. Khare, *Biomaterials*, 2020, **258**, 120280.

158 T. Wang, X. Zhang and D. D. Bikle, *J. Cell. Physiol.*, 2017, **232**, 913–921.

159 F.-C. Kao, P.-Y. Chiu, T.-T. Tsai and Z.-H. Lin, *Sci. Technol. Adv. Mater.*, 2019, **20**, 1103–1117.

160 J. Liu, B. Zhu, L. Zhang, J. Fan and J. Yu, *J. Colloid Interface Sci.*, 2021, **600**, 898–909.

161 A. T. Le, M. Ahmadipour and S.-Y. Pung, *J. Alloys Compd.*, 2020, **844**, 156172.

162 J. Wei, Y. Liu, Y. Li, Z. Zhang, J. Meng, S. Xie and X. Li, *Adv. Healthcare Mater.*, 2023, 2300338.

163 G. Tai, B. Reid, L. Cao and M. Zhao, in *Chemotaxis*, ed. T. Jin and D. Hereld, Humana Press, Totowa, NJ, 2009, vol. 571, pp. 77–97.

164 G. G. Genchi, E. Sinibaldi, L. Ceseracciu, M. Labardi, A. Marino, S. Marras, G. De Simoni, V. Mattoli and G. Ciofani, *Nanomedicine*, 2018, **14**, 2421–2432.

165 M. Sekkarapatti Ramasamy, V. Krishnamoorthi Kaliannagounder, A. Rahaman, C. H. Park, C. S. Kim and B. Kim, *ACS Biomater. Sci. Eng.*, 2022, **8**, 3542–3556.

166 D. Lei, N. Liu, T. Su, Q. Zhang, L. Wang, Z. Ren and Y. Gao, *Adv. Mater.*, 2022, **34**, 2110608.

167 D. Tan, C. Jiang, N. Sun, J. Huang, Z. Zhang, Q. Zhang, J. Bu, S. Bi, Q. Guo and J. Song, *Nano Energy*, 2021, **90**, 106528.

168 Y. Zhong, S. Huang, Z. Feng, Y. Fu and A. Mo, *J. Biomed. Mater. Res.*, 2022, **110**, 1840–1859.

169 J. Zhang, Y. Fu and A. Mo, *Int. J. Nanomed.*, 2019, **14**, 10091–10103.

170 S. H. Lee, S. Jeon, X. Qu, M. S. Kang, J. H. Lee, D.-W. Han and S. W. Hong, *Nano Convergence*, 2022, **9**, 38.

171 R. Nie, Y. Sun, H. Lv, M. Lu, H. Huangfu, Y. Li, Y. Zhang, D. Wang, L. Wang and Y. Zhou, *Nanoscale*, 2022, **14**, 8112–8129.

172 C. Buten, L. Kortekaas and B. J. Ravoo, *Adv. Mater.*, 2020, **32**, 1904957.

173 P. Mayorga-Burrezo, J. Muñoz, D. Zaoralová, M. Otyepka and M. Pumera, *ACS Nano*, 2021, **15**, 10067–10075.

174 I. De, P. Sharma and M. Singh, *Eur. J. Pharm. Biopharm.*, 2022, **173**, 73–91.

175 Y. Zhang, S. Chen, Z. Xiao, X. Liu, C. Wu, K. Wu, A. Liu, D. Wei, J. Sun, L. Zhou and H. Fan, *Adv. Healthcare Mater.*, 2021, **10**, 2100695.

176 L. F. Jaffe and M.-M. Poo, *J. Exp. Zool.*, 1979, **209**, 115–127.

177 N. Patel and M. Poo, *J. Neurosci.*, 1982, **2**, 483–496.

178 A. Kotwal, *Biomaterials*, 2001, **22**, 1055–1064.

179 Y. Shan, X. Cui, X. Chen and Z. Li, *Wiley Interdiscip. Rev.: Nanomed. Nanobiotechnol.*, 2023, **15**, e01827.

180 Y. Zhang, L. Zhou, X. Gao, C. Liu, H. Chen, H. Zheng, J. Gui, C. Sun, L. Yu and S. Guo, *Nano Energy*, 2021, **89**, 106319.

181 S. Vijayavenkataraman, *Acta Biomater.*, 2020, **106**, 54–69.

182 G. Viola, J. Chang, T. Maltby, F. Steckler, M. Jomaa, J. Sun, J. Edusei, D. Zhang, A. Vilches, S. Gao, X. Liu, S. Saeed, H. Zabalawi, J. Gale and W. Song, *ACS Appl. Mater. Interfaces*, 2020, **12**, 34643–34657.

183 A. C. Pinho, A. C. Fonseca, A. C. Serra, J. D. Santos and J. F. J. Coelho, *Adv. Healthcare Mater.*, 2016, **5**, 2732–2744.

184 M. Sarker, S. Naghieh, A. D. McInnes, D. J. Schreyer and X. Chen, *Biotechnol. J.*, 2018, **13**, 1700635.

185 Y. Qian, Y. Xu, Z. Yan, Y. Jin, X. Chen, W.-E. Yuan and C. Fan, *Nano Energy*, 2021, **83**, 105779.

186 S. Danti, B. Azimi, M. Candito, A. Fusco, M. S. Sorayani Bafqi, C. Ricci, M. Milazzo, C. Cristallini, M. Latifi, G. Donnarumma, L. Bruschini, A. Lazzeri, L. Astolfi and S. Berrettini, *Biointerphases*, 2020, **15**, 031004.

187 E. Esmaeili, M. Soleimani, M. A. Ghiass, S. Hatamie, S. Vakilian, M. S. Zomorrod, N. Sadeghzadeh, M. Vossoughi and S. Hosseinzadeh, *J. Cell. Physiol.*, 2019, **234**, 13617–13628.

188 K. Wang, Y. Jia and X. Yan, *Nano Energy*, 2022, **100**, 107486.

189 Y. Li, Y. Hu, H. Wei, W. Cao, Y. Qi, S. Zhou, P. Zhang, H. Li, G.-L. Li and R. Chai, *J. Nanobiotechnol.*, 2022, **20**, 398.

190 M. Xiao, X. Li, S. Pifferi, B. Pastore, Y. Liu, M. Lazzarino, V. Torre, X. Yang, A. Menini and M. Tang, *Nanoscale*, 2022, **14**, 10992–11002.

191 A. Gustavsson, P. Brinck, N. Bergvall, K. Kolasa, A. Wimo, B. Winblad and L. Jönsson, *Alzheimer's Dementia*, 2011, **7**, 318–327.

192 D. Eleftheriadou, D. Kesidou, F. Moura, E. Felli and W. Song, *Small*, 2020, **16**, 1907308.

193 Y. Jin, J. Seo, J. S. Lee, S. Shin, H.-J. Park, S. Min, E. Cheong, T. Lee and S.-W. Cho, *Adv. Mater.*, 2016, **28**, 7365–7374.

194 D. Zhao, P. Feng, J. Liu, M. Dong, X. Shen, Y. Chen and Q. Shen, *Adv. Mater.*, 2020, **32**, 2003800.

195 R. Yamaji, K. Fujita, S. Takahashi, H. Yoneda, K. Nagao, W. Masuda, M. Naito, T. Tsuruo, K. Miyatake, H. Inui and Y. Nakano, *Biochim. Biophys. Acta, Mol. Cell Res.*, 2003, **1593**, 269–276.

196 F. Lavini, A. Calò, Y. Gao, E. Albisetti, T.-D. Li, T. Cao, G. Li, L. Cao, C. Aruta and E. Riedo, *Nanoscale*, 2018, **10**, 8304–8312.

197 C. Giuliani, *Antioxidants*, 2019, **8**, 112.

198 N. Gao, J. Zhao, X. Zhu, J. Xu, G. Ling and P. Zhang, *Acta Biomater.*, 2022, S1742706122006614.

199 G. Li, Y. Fan, L. Lin, R. Wu, M. Shen and X. Shi, *Sci. China: Chem.*, 2021, **64**, 817–826.

200 S. Lin, X. Hu, J. Lin, S. Wang, J. Xu, F. Cai and J. Lin, *Analyst*, 2021, **146**, 4391–4399.

201 Y. Nie, W. Zhang, W. Xiao, W. Zeng, T. Chen, W. Huang, X. Wu, Y. Kang, J. Dong, W. Luo and X. Ji, *Biomaterials*, 2022, **289**, 121791.

202 H. Zhang, H. Yang, P. Liu, X. Qin and G. Liu, *Talanta*, 2022, **237**, 122906.

203 A. Ahmadi, S. M. Khoshfetrat, S. Kabiri, P. S. Dorraji, B. Larijani and K. Omidfar, *Microchim. Acta*, 2021, **188**, 296.

204 N. Gong, Y. Zhang, X. Teng, Y. Wang, S. Huo, G. Qing, Q. Ni, X. Li, J. Wang, X. Ye, T. Zhang, S. Chen, Y. Wang, J. Yu, P. C. Wang, Y. Gan, J. Zhang, M. J. Mitchell, J. Li and X.-J. Liang, *Nat. Nanotechnol.*, 2020, **15**, 1053–1064.

205 Q. Ouyang, B. Wang, W. Ahmad, Y. Yang and Q. Chen, *Anal. Bioanal. Chem.*, 2022, **414**, 8179–8189.

206 R. Ye, H. Chen and H. Li, *Anal. Chim. Acta*, 2022, **1225**, 340227.

207 L. Vannozzi, L. Ricotti, C. Filippeschi, S. Sartini, V. Coviello, V. Piazza, P. Pingue, C. La Motta, P. Dario and A. Menciassi, *Int. J. Nanomed.*, 2015, 69.

208 Y. Ma, L. Jiang, J. Hu, E. Zhu and N. Zhang, *ACS Appl. Mater. Interfaces*, 2022, **14**, 44065–44083.

209 D. Huang, T. Wu, S. Lan, C. Liu, Z. Guo and W. Zhang, *Biomaterials*, 2022, **289**, 121808.

210 B. Li, G. Hao, B. Sun, Z. Gu and Z. P. Xu, *Adv. Funct. Mater.*, 2020, **30**, 1909745.

211 M. Coluccia, V. Parisse, P. Guglielmi, G. Giannini and D. Secci, *Eur. J. Med. Chem.*, 2022, **244**, 114801.

212 S. Zheng, Y. Tian, J. Ouyang, Y. Shen, X. Wang and J. Luan, *Front. Chem.*, 2022, **10**, 990362.

213 D. V. Shtansky, A. T. Matveev, E. S. Permyakova, D. V. Leybo, A. S. Konopatsky and P. B. Sorokin, *Nanomaterials*, 2022, **12**, 2810.

214 K. Vimala, K. Shanthi, S. Sundarraj and S. Kannan, *J. Colloid Interface Sci.*, 2017, **488**, 92–108.

215 C. Mo, Z. Wang, J. Yang, Y. Ouyang, Q. Mo, S. Li, P. He, L. Chen and X. Li, *J. Photochem. Photobiol., B*, 2022, **233**, 112487.

216 T. Hu, Z. Gu, G. R. Williams, M. Strimaite, J. Zha, Z. Zhou, X. Zhang, C. Tan and R. Liang, *Chem. Soc. Rev.*, 2022, **51**, 6126–6176.

217 H. Zhao, S. Xue, M.-D. Hussherr, A. P. Teixeira and M. Fussenegger, *Sci. Adv.*, 2022, **8**, eabm4389.

218 Z. Liu, J. Nie, B. Miao, J. Li, Y. Cui, S. Wang, X. Zhang, G. Zhao, Y. Deng, Y. Wu, Z. Li, L. Li and Z. L. Wang, *Adv. Mater.*, 2019, **31**, 1807795.

219 E. Abu-El-Rub, R. R. Khasawneh and F. Almahasneh, *World J. Stem Cells*, 2022, **14**, 513–526.

220 M. Jeong, Y. Jung, J. Yoon, J. Kang, S. H. Lee, W. Back, H. Kim, M. J. Sailor, D. Kim and J.-H. Park, *ACS Nano*, 2022, **16**, 16118–16132.

221 N. Muzzio, M. Eduardo Martinez-Cartagena and G. Romero, *Adv. Drug Delivery Rev.*, 2022, **190**, 114554.

222 C. Pucci, A. Marino, Ö. Şen, D. De Pasquale, M. Bartolucci, N. Iturrioz-Rodríguez, N. di Leo, G. de Vito, D. Debellis, A. Petretto and G. Ciofani, *Acta Biomater.*, 2022, **139**, 218–236.

223 Y. Chen, B. Ma, X. Wang, X. Zha, C. Sheng, P. Yang and S. Qu, *J. Diabetes Res.*, 2021, **2021**, 1–10.

224 J. Zhuang, X. Zhang, Q. Liu, M. Zhu and X. Huang, *Theranostics*, 2022, **12**, 6223–6241.

225 Y. Qiao, W. Zhang, P. Tian, F. Meng, H. Zhu, X. Jiang, X. Liu and P. K. Chu, *Biomaterials*, 2014, **35**, 6882–6897.

226 S. Lin, S. Yin, J. Shi, G. Yang, X. Wen, W. Zhang, M. Zhou and X. Jiang, *Bioact. Mater.*, 2022, **18**, 116–127.

227 Q. Wu, L. Hu, R. Yan, J. Shi, H. Gu, Y. Deng, R. Jiang, J. Wen and X. Jiang, *Bone Res.*, 2022, **10**, 55.

228 X. Yao, S. Lu, C. Feng, R. Suo, H. Li, Y. Zhang, Q. Chen, J. Lu, B. Wu and J. Guo, *Biomaterials*, 2022, **289**, 121801.

229 M. Mathesh, B. Luan, T. O. Akanbi, J. K. Weber, J. Liu, C. J. Barrow, R. Zhou and W. Yang, *ACS Catal.*, 2016, **6**, 4760–4768.

230 A. S. Timin, A. R. Muslimov, M. V. Zyuzin, O. O. Peltek, T. E. Karpov, I. S. Sergeev, A. I. Dotsenko, A. A. Goncharenko, N. D. Yolshin, A. Sinelnik, B. Krause, T. Baumbach, M. A. Surmeneva, R. V. Chernozem, G. B. Sukhorukov and R. A. Surmenev, *ACS Appl. Mater. Interfaces*, 2018, **10**, 34849–34868.

231 G.-H. Feng and W.-M. Tseng, *IEEE Sens. J.*, 2018, **18**, 9736–9743.

232 Y. Zhang, Q. An, W. Tong, H. Li, Z. Ma, Y. Zhou, T. Huang and Y. Zhang, *Small*, 2018, **14**, 1802136.

233 Y. Zhang, C. Tong, Z. Ma, L. Lu, H. Fu, S. Pan, W. Tong, X. Li, Y. Zhang and Q. An, *Nanoscale*, 2019, **11**, 14372–14382.

234 Q. Liang, J. Xi, X. J. Gao, R. Zhang, Y. Yang, X. Gao, X. Yan, L. Gao and K. Fan, *Nano Today*, 2020, **35**, 100935.

235 Y. Wang, Q. Tang, R. Wu, S. Sun, J. Zhang, J. Chen, M. Gong, C. Chen and X. Liang, *ACS Nano*, 2023, **17**, 3557–3573.